Solar Physics

Kuramoto Model with non-symmetric coupling reconstructs variations of the solar cycle period

--Manuscript Draft--

Manuscript Number:	SOLA-D-15-00166R2
Full Title:	Kuramoto Model with non-symmetric coupling reconstructs variations of the solar cycle period
Article Type:	Original Research
Keywords:	"Solar cycle": "Nonlinear oscillators"; "Solar Activity"; "Kuramoto model"; "Geomagnetic indices"; "Coupling"; "Phase synchronization"
Corresponding Author:	Elena Blanter Institut de Physique du Globe de Paris Paris, FRANCE
Corresponding Author Secondary Information:	
Corresponding Author's Institution:	Institut de Physique du Globe de Paris
Corresponding Author's Secondary Institution:	
First Author:	Elena Blanter
First Author Secondary Information:	
Order of Authors:	Elena Blanter
	Jean-Louis Le Mouël
	Mikhail Shnirman
	Vincent Courtillot
Order of Authors Secondary Information:	
Funding Information:	Institute de Physique du Globe — Not applicable
Abstract:	We apply a Kuramoto model with two non-linear coupled oscillators to the simultaneous reconstruction of the phase difference of the two oscillators and instantaneousaneous period (or length) of the solar cycle. The two long series of sunspot numbers [RI] and aa geomagnetic indices are considered as proxies of the toroidal and poloidal components of the solar magnetic field, respectively. Variations in the length of the solar cycle are successfully reconstructed when a dissymmetry between coupling coefficients is introduced, corresponding to a dissymmetry of the αΩ-mechanisms of solar magnetic-field generation. Application of the Kuramoto model to solar indices and comparison with synthetic data series shows the important role of synchronization in allowing one to estimate solar-cycle length. The Kuramoto model reconstruction reveals a ≈30-33 year (three solar cycles) quasi-periodicity and the influence of quasi-biennial oscillations present in the aa-index on the determination of solar-cycle length.

Dear Editor,

we hereby submit the revision of our paper "Kuramoto Model with non-symmetric coupling reconstructs variations of the solar cycle period" (Authors: E. Blanter, J.-L Le Mouël, M. Shnirman and V. Courtillot; manuscript SOLA-D-15-00166).

We are extremely thankful to the referee for his/her very useful comments, that we have attempted to answer. We believe we have successfully done so for all of them. Particularly notable was the remark on the neglect of amplitude and shape of the solar cycles. This led us to additional modeling and the demonstration (that had not been done in our original paper) that these could indeed be neglected and that our conclusions remained unchanged if they were included. This has led to a new paragraph in the discussion section (6) and to a new appendix.

Our more detailed responses are given below after each of the referee's comments (reproduced in italics).

This article is a follow up of a previous work of the same authors Blanter et al.(2014) about using a reconstruction method to infer the variations of the solar period cycle. In this new article the authors study non-symmetric coupling, a more realistic approach than symmetric coupling used in the previous publication. The results found are of interest to the solar physics community, and for that reason I recommend its publication. Nevertheless, there are several points that the authors should address before the manuscript is ready for publication.

[In the report - new references are quoted by their ads numbers such as2010LRSP....7....3C if applicable. To access the articlehttp://adsabs.harvard.edu/abs/2010LRSP....7....3C]

The article should be carefully read, the figure numbers checked and the captions improved.
Done.

There are figures without a correct label and there is a figure missing.
Corrected.

Main Points that the authors should address:

- The article focuses on an inversion method of the solar cycle period based on the possible synchronization between oscillators, assumed to describe the time variation of the toroidal and poloidal components of the solar magnetic field. The authors should justify better why these two components of the solar magnetic field can be assumed to behave as such, see 2010LRSP....7....3C and references therein.

This is now done in several parts of the manuscript. The introduction has been entirely re-written in order to answer this and other questions as indicated below. New references as indicated by the referee have been quoted and added to the reference list.

- The use of international SSN and aa-index as proxies of the toroidal and poloidalcomponents of the solar magnetic field is much disputed. The point is discussed inLopes et al. (2014, 2014SSRv..186..535L), Petrovay (2010, 2010LRSP....7....6P),Usoskin (2013, 2013LRSP...10....1U) and Usoskin (2013, 2013LRSP...10....1U) Vieiraand Solanki (2010, 2010A&A...509A.100V) Svalgaard, L.; Cliver (2007,2007AdSpR..40.1112S). These points should be addressed in the introduction.

Done. We quote several of these papers and point out remaining controversies such as between Petrovay (2010) and Lopes et al (2014).

-Justify and explain why it is valid to make the hypotheses that the amplitude and shape of the solar cycle do not change, although, it is necessary to apply the Kuramoto Model, this seems very unrealistic for the real Sun. Can the authors explain why this can be done, what are the caveats and estimate the error introduced by making this strong hypothesis in the inversion method.

As mentioned above, we have now explicitly studied this problem (for amplitude; shape changes have even a smaller effect) and come to the conclusion that indeed our conclusions remain when amplitude (and shape) are taken into account (paragraph 6.1 and appendix added).

- The study is based on the coupling of two oscillators as representing the coupling between the poloidal and toroidal components of the magnetic field, however solar dynamo suggests that components of the magnetic field behave like a Van der Pol oscillator (Lopes et al. ,2014, 2014SSRv..186..535L). Explain why the approximation by two oscillators is possible.

Indeed, time series produced by solar dynamo theory (under some definite assumptions) are compatible with the suggestion that components of the magnetic field behave like a Van der Pol oscillator; this is a fruitful method of investigation of solar activity (see f. i. the nice work of Lopes, 2014). But this Van der Pol oscillator approximation is not sufficient. Indeed, one can use only one magnetic field component in an inversion, when in reality we have at least two components (see f.i. many papers on solar cycle predictions that used also the *aa*-index for ISSN predictions).

In our paper, we are interested in the interaction between these two components.

As to Kuramoto modeling of this interaction between field components and its link with the equations of physics, we insist that the Kuramoto model is not (and does not have to be in order to be useful) an explicit approximation of MHD equations. We try to express an interaction between two field components in the simplest form. This may be called a "toy model" of the interaction between magnetic field components. The two couplings in our model are given in a “kinematic” way (we assume that they can be described by given movements of the solar plasma).These two couplings are not equal to one another because the motions (circulation)that create them are different. One of the couplings is due to the motion that creates the toroidal component from the poloidal one and the other coupling is due to the motion that creates the poloidal component from the toroidal one.

Review of the different sections:

(1) Introduction, page 2, lines 38-44: "To avoid the full complexity of solar cycle properties, we restrict our investigation to the evolution of the instantaneous period of the 11 year solar cycle, ignoring the amplitude and shape of the cycle." - This is a strong constraint imposed by the method, the authors should explain the interest of the work, since this approximation is very strong – it relates to one of the main points to be addressed in the article.

Done, as written above. We therefore show that Kuramoto modeling is a reasonable approach to the problem of interaction of phase components of the solar cycle.

(2) Introduction, page 2, lines 9-17: "We applied a Kuramoto model with two oscillators and an evolving symmetric coupling to the inverse problem of the reconstruction of the correlation between relevant solar indices (Blanter et al.2014). In the present paper, in addition, we solve the inverse problem of the reconstruction of the solar cycle period length." The fact that the authors do not take into account the variation of the amplitude and shape of the solar cycle, causes the model to

have a very limited used. The authors should give some motivation (based in solar dynamo) to strengthen the argument of evolving symmetric coupling.

Done, as written above.

(3) Introduction, page 3, lines 36-46 "This dissymmetry between oscillators could be the signature of a dissymmetric feedback of one field component on the other. We find that it is a requisite if one wants to generate variations in the cycle length." Dissymmetry is a very important property of this Kuramoto Model in this study, the authors must justify (based in dynamo theory) this better.

Done, as written above. We point out the very different mechanisms which create poloidal field from toroidal and vice-verse (and add references). We add that these very mechanisms provide us with linkages between the phases of the toroidal and poloidal components.

(4) In the introduction, the authors should make reference to the large number of researchers working on Kuramoto models (see the review of Acebrón et al. 2005RvMP...77..137A)

We have quoted several references on this point, the most complete being Acebron (2005) that investigates cases with constant coupling (and a very large number of oscillators).

(5) In the introduction, the authors should make reference to solar dynamosmodels/inversion methods for which much of this study will be of great interest. Inparticular see the articles: 2008SoPh..250..403P,2009SoPh..257....1L,2009MNRAS.397..320L,2012SoPh..278..137K,2012PhRvL.109q1103C, 2013AN....334..964N, 2015SoPh..290.1851H.

Done.

(6)3.2 Quality of the reconstruction: Figure 1 and 2 seem to be incorrectly labeled, please correct.

Done.

(7) 3.2 Quality of the reconstruction, page 3, lines 2-6: "Their amplitude varies because the varying correlation . . . according to Eq. (9)." In figure 1 (actually figure 2) there is an amplitude variation. I am curious to see how this effect is discussed for the real data for which the amplitude variation is significant as shown in observations and numerical dynamo simulations/models. It could be interesting to study the impact of the solar noise on this curve to estimate the validity of the method. Equally the authors can make a simulation of amplitude variation using a synthetic time series to estimate how the hypothesis of fixed amplitude affects the final result.

As already said emphatically, this was an excellent suggestion. We performed the required simulations and obtained two important results:

1) The amplitude variation observed in the solar cycle is not sufficient to generate the solar cycle period variation.

2) The Kuramoto model does not represent well the variations of the period that are generated by variations of the amplitude, and the quality of the reconstruction in such models is worse than that of real data (observations). So, we think that real observations result essentially from period, not amplitude oscillations.

In the new version, we have included an Appendix with examples and we refer to these results in the discussion (section 6.1).

(8) 3.2 Quality of the reconstruction, page 3, lines 35-39: "High-frequency noise on the correlation curve at Figure 2a is due to the influence of varying period to the estimation of the

phase difference." The authors should check if the experimental error could affect the result, once it is possible to compute the error for the aa and SSN time series, it is interesting to see if the inversion of figure 2a is affected by it and how. Moreover as the SSN the daily time series has great volatility. What will happen to this inversion if such observational error is assumed in this type of inversions? As mentioned previously the authors could use the synthetic time series to test the method for amplitude and noise variations on the reconstruction technique.

The questions of quality of the reconstruction of **correlation** and impact of **daily noise** have already been discussed in our previous papers: Blanter et al, 2014 (2014SoPh..289.4309B, 2014JASTP.117...71B) and Le Mouel et al 2012JGRA..117.9103L. The present paper addresses the reconstruction of the **instant period**. In the new version, we have added a section concerning the impact of daily noise on the amplitude in section A2 of the new Appendix.

(9) The caption of figure 3 is incomplete: what is the meaning of the green curve ?

See next comment.

(10) "4.2. The instant period of the solar cycle", page:11, line 26-27: Figure 4 is exactly the same as figure 5. "Resulting curves of the instant periods are presented in Figure 4." Must be replaced.

In the previous version, Figure 5 was submitted twice erroneously. Figure 3 was erroneously omitted and Figure 4 took its place. Figures have been checked in the new version. We thank the reviewer for pointing this out.

(11) "4.2. The instant period of the solar cycle ". This is not directly related with the work (which use annual averages), but could be interesting to address theimpact of daily SSN on the reconstructs of the variation of the solar cycle period. Since, until now short time scale variations of solar time series have not been fully addressed (for example see the recent article 2015ApJ...804..120L).

Short term variations of the amplitude and their impact on the reconstruction of the solar cycle period are now addressed in the new version in section A2 of Appendix.

(12) "5. Application of Kuramoto model to solar indices": Figure 5, captures the main result of the article. Although the result is interesting, its relevance for understanding the properties of the evolution of solar magnetic is not fully addressed. The authors should highlight the relation that exists between the paper's result and what is obtained currently by recent dynamo models, see the reviews from Karak et al. (2014,2014SSRv..186..561K).

Done. We now write about the possible role of the amplitude of meridional flow, which on one hand provides an important connection between toroidal and poloidal field components and on the other hand strongly affects the period length (see Karak).

(13) "5.4. Effect of preliminary averaging". Figure 6d shows a clear dependence of Lo averaging. Does this not strongly limit the conclusion about the inversion method?

No, as is now discussed in section 6.3, where we conclude that quasi-biennial oscillations affect the determination of the solar cycle period in the aa-index but do not affect its long-term correlation with sunspot number.

(14) "5.5. Toroidal and poloidal components of the solar magnetic field". page 15,lines 22-28:"On the plot of reconstructed correlation (Figure 8c, red curve) the sign reversal is evident. For the two non-linear oscillators this reversal means a change of leading oscillator." This could be an

interesting result. Can this be attributed to a solar dynamo physical process or an anomaly in the record data ?

This question was addressed in our previous paper (2014SoPh..289.4309B). In the present work, we only refer to previous results.

(15) 5.6 Effect of de-correlation on the reconstruction of the instant period page15, lines 40-43:" In contrast to the high correlation between the RI and aa indices at the beginning of the graph (Figure 5c), the corresponding correlation between the RI and aap indices is close to zero (Figure 8c). " This is quite interesting. Can the authors give a reason for that based on the mathematical structure of the Kuramoto Model ?

This is not a question of Kuramoto model but due to the definition of the aa_p index. The linear coefficients in Eq. (19) were chosen to obtain an index that does not depend on SSN (Ruzmaikin and Feynman, 2001).

(16) 6. Discussion and conclusions: " Let us note that, in terms of a solar dynamo, the lack of symmetry between the poloidal and the toroidal magnetic field components seems to be a more natural assumption than the symmetric coupling considered in Blanter et al, (2014)". I agree, but it could be interesting if the authors can use solar dynamo theory (observations and numerical simulations to argue this point -see publications mentioned previously).

Done, as written several times above.

(17) 6. Discussion and conclusions: The conclusion addresses well the interest and many implications of this research work, however, some of the points discussed previously could be address briefly in this section in order to strengthen the quality of the results obtained.

Done.

Kuramoto Model with Non-Symmetric Coupling Reconstructs Variations of the Solar Cycle Period.

E. Blanter[1,2], J.-L Le Mouël[2], M. Shnirman[1,2], V. Courtillot[2]

blanter@ipgp.fr

[1]*IEPT RAS, Profsoyuznaya str. 84/32, 117997, Moscow, Russia*

[2]*Institut de Physique du Globe, Sorbonne Paris Cité, Paris, France*

Abstract

We apply a Kuramoto model with two non-linear coupled oscillators to the simultaneous reconstruction of the phase difference of the two oscillators and instantaneousaneous period (or length) of the solar cycle. The two long series of sunspot numbers [R_I] and aa geomagnetic indices are considered as proxies of the toroidal and poloidal components of the solar magnetic field, respectively. Variations in the length of the solar cycle are successfully reconstructed when a dissymmetry between coupling coefficients is introduced, corresponding to a dissymmetry of the αΩ-mechanisms of solar magnetic-field generation. Application of the Kuramoto model to solar indices and comparison with synthetic data series shows the important role of synchronization in allowing one to estimate solar-cycle length. The Kuramoto model reconstruction reveals a ≈30–33 year (three solar cycles) quasi-periodicity and the influence of quasi-biennial oscillations present in the aa-index on the determination of solar-cycle length.

1. Introduction

The cyclic nature of sunspot activity is due to the cyclic regeneration of the large-scale magnetic field of the Sun. The Sun's magnetic cycle is produced by a dynamo process, which is based on the nonlinear interaction between the velocity field and the magnetic field in the solar plasma (Karak *et al*. 2014). The basic idea of the αΩ-dynamo is that the toroidal and the poloidal fields sustain each other through a feedback loop. The poloidal field can be stretched by the differential rotation to produce the toroidal field. The turbulence in the solar convection zone twists the toroidal field to produce the poloidal field. The latter mechanism is known as the α-effect and despite wide investigations it is still poorly understood. The full differential equations of magnetohydrodynamics (MHD) are easily written but are difficult to solve under realistic assumptions. Various attempts to simplify these equations in order to get a solution led to a wide class of kinematic models (see review by Karak *et al*. 2014). Kinematic models, *e.g.* Flux-Transport dynamo (FTD) models, allow to investigate how distinct physical processes, such as fluctuations in poloidal-field generation or variations in meridional circulation, influence properties of the solar cycle (Karak *et al.* 2014; Hazra *et al*. 2015).

The full MHD equations and even their kinematic simplification (FTD) are too complex to allow a unique solution of the inverse problem. An alternate approach consists in using models with non-linear oscillators that use simplified parameterizations of the main physical mechanisms of the dynamo process. Although in the Sun's interior the magnetic field generated by the dynamo has a very rich and complex structure, several properties of the cycle can be understood by analyzing solutions of low-order differential equations (Lopes *et al*. 2014). For example, applying the axisymmetric simplification allows one to write a Van der Pol differential equation describing the evolution of the toroidal component of the solar magnetic field (Nagy and Petrovay, 2006; Lopes *et al*. 2014); the evolution of the poloidal component is not considered in this approach. The simple equations of Low-Order Differential Models (LODM) allow the application of inverse methods. In our approach, we try to combine the

advantages of LODM with the simultaneous consideration of both magnetic-field components (toroidal and poloidal) present in FTD models. The Kuramoto model of two non-linear coupled oscillators successfully reconstructs the phase evolution of both the poloidal and toroidal components of the solar magnetic field (Blanter *et al*. 2014) and allows the application of inverse methods. In that paper, for the sake of simplicity, we did not consider the evolution of the amplitude of the solar cycle; however, as we shall show in the present article, the contribution of the amplitude variations to the variability of solar cycle length can be considered separately (see Appendix). The main advantage of the Kuramoto model consists in its schematic representation of the couplings of the poloidal and toroidal components of the solar field, which is a key element of all solar dynamos (Charbonneau, 2010), although there is as yet no consensus on the details and respective intensities of these couplings.

Long series of solar indices reveal irregularities in the ≈11-year long Schwabe cycle. The solar cycle duration typically ranges between 10 and 12 years with the full range of variations going from 7 to 17 years (Richards, Rogers, Richards, 2009). Departures of solar activity from a regular periodic process (Hathaway, 2015) are of paramount importance in trying to understand and unravel the complex solar dynamo. An $\alpha\Omega$ solar dynamo (Charbonneau, 2010) can produce a variability in both the solar cycle length and amplitude (*e.g.* the Gnevyshev–Ohl rule of odd and even solar cycles), as well as an asymmetric rise–fall profile of the sunspot cycle. In the present work we focus on the phase origin of variations in solar cycle duration and we apply inversion methods.

The Kuramoto model of nonlinear coupled oscillators was initially considered for the study of synchronization and phase locking in complex systems (Acebron *et al*. 2005). Usually, a system with a large number [N] of oscillators is used and the solution is studied in the limit case of infinite [N] (Strogatz, 2000). However, recently, it was found that the Kuramoto model with a small number of oscillators (N from 3 to 5) also produces interesting features and chaotic dynamics (Popovych, Maistrenko, Tass, 2005; Ashwin, Burylko, Maistrenko, 2008; Tilles, Cerdeira, Ferreira, 2013). The case of two oscillators with constant symmetrical coupling was

fully described by Dorfler and Bullo (2011, 2014). The first attempts to study Kuramoto models with an evolving coupling was done for a particular form of coupling in a system of four oscillators (Cumin and Unsworth, 2007). A Kuramoto model with two coupled oscillators and an evolving symmetric coupling successfully reproduces the long-term evolution of the correlation between the toroidal and poloidal components of the solar magnetic field, represented by the sunspot number [R_I] and aa-indices respectively (Blanter *et al*. 2014). The couplings between the toroidal and poloidal magnetic-field components used in that article were assumed to be the same (symmetric coupling is usually considered in Kuramoto models), and the frequency of the oscillators was taken to be constant. In the present article we assume the two couplings to be different. This assumption naturally follows from differences between mechanisms of generation of poloidal and toroidal solar magnetic fields. The dissymmetry between the two couplings generates deviations from the mean frequency, *i.e.* variations in the length of the cycle period.

The Kuramoto model ignores the amplitude variation of the magnetic field and focuses on the frequency domain. This approach makes it a simple "toy model" with a small number of free parameters that allows solving an inverse problem (Section 2.3) when the two coupled oscillators are well-synchronized. The two differential equations of the Kuramoto model do not follow from a simplification of MHD equations, as is the case for kinematic models and models based on the Van der Pol–Dufing differential equation (*e.g.* Passos and Lopes, 2008). Therefore, one cannot estimate model parameters from observable physical values and one must solve the inverse problem mathematically. Nevertheless, the couplings in our Kuramoto model may be considered as a global representation of the physical processes involved in poloidal and toroidal magnetic field generation. They allow one to distinguish between poloidal to toroidal and toroidal to poloidal feedbacks but not to separate the effects of mechanisms such as meridional circulation or diffusion. Recent results concerning possible origins of solar cycle length variations obtained in FTD (Karak *et al*. 2014) and Van der Pol oscillator (Lopes *et al*. 2014)

models may be associated with the evolution of the coupling in the Kuramoto model (see Section 6 for details).

Following Blanter *et al.* (2014), we consider the sunspot number [R_I] and aa-indices as representative series of the toroidal and poloidal magnetic field. Links between the sunspot number index and the solar magnetic field have been much debated (see, *e.g.,* Svaalgard and Cliver, 2007; Vieira and Solanki, 2010; Usoskin, 2013; Lopes *et al*. 2014). However, applying the Kuramoto model, we could recover only the phase information and had to ignore variations in amplitude. From this point of view, all indices based on sunspot observations (sunspot number, areas, groups) may be considered as equivalent. The advantage of the sunspot-number series compared to the surface magnetic flux, radio flux, solar wind, coronal, or solar-flare indices consists in its quality and the long history of its regular observations. We restrict our analysis to the period during which the aa-index is also available (that is since 1868) and avoid periods of Grand Minima, when the lack of sunspots allows only a poor representation of the evolution of the solar magnetic field (Usoskin, 2013). The only difference between indices that could affect our reconstructions is the level of noise affecting the ≈11-year frequency domain: we average observations over a one-year sliding window, and thus we reduce the high-frequency noise in the data series. However, the medium range periodicities on the order of one to several years unfortunately cannot be avoided: we discuss their possible influence on the results.

In the present article, in which we introduce coupling dissymmetry, we ignore at first variations in amplitude and shape of solar cycles; we address the corresponding limitations in the discussion section and appendix. The article is organized as follows: in Section 2, we present the Kuramoto model with two nonlinear oscillators and non-symmetric coupling, and describe its properties on model examples in Section 3. Solar indices are described in Section 4 and the phase and mean length of the solar cycle are reconstructed by the Kuramoto model in Section 5. Results are discussed and summarized in Section 6.

2. Kuramoto Model with Two Oscillators and Non-Symmetric Coupling

The simplest Kuramoto model (KM) determines the evolution of the phases of two oscillators by a system of differential equations, and it does not treat the frequency or the amplitude of the oscillations. In Blanter *et al*. (2014) the coupling [$\kappa(t)$] between the two oscillators entered symmetrically in the two differential equations governing the evolution of the phases, and the frequency of the oscillations was determined by a given base frequency [Ω]. In the present article we obtain variations of the period of the oscillations by allowing the coupling to have a different action on each oscillator.

2.1. Coupling and Phase Evolution

As in Blanter *et al*. (2014), we consider two coupled oscillators with given frequencies $\omega_1 = \Omega + \Delta\omega$ and $\omega_2 = \Omega - \Delta\omega$. The temporal evolutions of their respective phases [$\theta_1(t)$ and $\theta_2(t)$] are governed by the system of non-linear differential equations:

$$\begin{aligned} \dot{\theta}_1 &= \omega_1 + \frac{\kappa_1}{2}\sin(\theta_2 - \theta_1) \\ \dot{\theta}_2 &= \omega_2 + \frac{\kappa_2}{2}\sin(\theta_1 - \theta_2) \end{aligned} \qquad (1)$$

Denoting the mean coupling as $\kappa(t) = \frac{\kappa_1(t) + \kappa_2(t)}{2}$ and the coupling dissymmetry as $\Delta\kappa(t) = \frac{\kappa_1(t) - \kappa_2(t)}{2}$, we rewrite Equation (1) in the form:

$$\begin{aligned} \dot{\theta}_1 &= \Omega + \Delta\omega + \frac{\kappa + \Delta\kappa}{2}\sin(\theta_2 - \theta_1) \\ \dot{\theta}_2 &= \Omega - \Delta\omega + \frac{\kappa - \Delta\kappa}{2}\sin(\theta_1 - \theta_2) \end{aligned} \qquad (2)$$

The sum and difference of the two differential equations yield:

$$\begin{aligned} \frac{\dot{\theta}_1 + \dot{\theta}_2}{2} &= \Omega - \frac{\Delta\kappa}{2}\sin(\theta_1 - \theta_2) \\ \dot{\theta}_1 - \dot{\theta}_2 &= 2\Delta\omega - \kappa\sin(\theta_1 - \theta_2) \end{aligned} \qquad (3)$$

Let $\theta(t)=\theta_1(t)-\theta_2(t)$ stand for the phase difference, and $\omega(t)=\frac{\dot{\theta}_1(t)+\dot{\theta}_2(t)}{2}$ be called the instantaneousaneous frequency. It follows from Equation (3):

$$\omega(t)=\Omega-\frac{\Delta\kappa(t)}{2}\sin\left(\theta(t)\right) \tag{4}$$

$$\dot{\theta}(t)=2\Delta\omega-\kappa(t)\sin\left(\theta(t)\right) \tag{5}$$

2.2. Phase Difference and Sliding Correlation

The sliding correlation between two sine functions with constant frequency $X_0(t)=\sin\left(\Omega t-\frac{\varphi}{2}\right)$ and $Y_0(t)=\sin\left(\Omega t+\frac{\varphi}{2}\right)$ taken over a time interval of length $\Theta=\frac{2\pi}{\Omega}$ centered at *t* is given by the phase difference [φ]:

$$C_0(t)=C_\Theta\left(X_0(t),Y_0(t)\right)=\cos(\varphi) \tag{6}$$

When two series $X_0(t)=\sin\left(\theta_1(t)\right)$ and $Y_0(t)=\sin\left(\theta_2(t)\right)$ oscillate with slowly varying frequencies $\dot{\theta}_1(t)$ and $\dot{\theta}_2(t)$ and the mean frequency $\omega_0(t)=\frac{\dot{\theta}_1(t)+\dot{\theta}_2(t)}{2}$ is close to Ω, then their sliding correlation taken over the interval $\Theta=\frac{2\pi}{\Omega}$ is also determined by the phase difference $\theta(t)=\theta_1(t)-\theta_2(t)$:

$$C_0(t)=C_\Theta\left(X_0(t),Y_0(t)\right)=\cos\left(\theta(t)\right) \tag{7}$$

Equation (7) gives a relationship between the evolution of the phase difference between two oscillating series and their sliding correlation under the condition of a slow frequency evolution. We have used this relationship to solve the inverse problem applying the Kuramoto model with symmetric coupling in Blanter et al. (2014).

2.3. Inverse Problem

Let us recall that the use of the sliding correlation in Equations (8) and (9) for the estimation of the phase difference $\theta(t)$ is legitimate in the assumption of slowly evolving $\theta(t)$ and coupling dissymmetry [$\Delta\kappa(t)$].

Let us now start with two series $X_0(t)=\sin(\varphi_1(t))$ and $Y_0(t)=\sin(\varphi_2(t))$ and investigate whether phases $\theta_1(t)$ and $\theta_2(t)$ generated by a Kuramoto model represent well the initial phases $\varphi_1(t)$ and $\varphi_2(t)$. For that, we estimate the correlation $C_0(t)$ and the instantaneous frequency $\omega_0(t)$, and resolve Equations (4)-(7) to determine the mean coupling $\kappa(t)$ and the coupling dissymmetry $\Delta\kappa(t)$:

$$\kappa(t)=\frac{2\Delta\omega-\left(\arccos\left(C_0(t)\right)\right)'}{\sin\left(\arccos\left(C_0(t)\right)\right)} \tag{8}$$

$$\Delta\kappa(t)=\frac{2\left(\Omega-\omega_0(t)\right)}{\sin\left(\arccos\left(C_0(t)\right)\right)} \tag{9}$$

We substitute the so obtained $\kappa(t)$ and $\Delta\kappa(t)$ into Equation (2), obtain phases $\theta_1(t)$ and $\theta_2(t)$ and simulate two model series $X(t)=\sin(\theta_1(t))$ and $Y(t)=\sin(\theta_2(t))$. The closeness of the sliding correlation $C(t)=C_\Theta(X,Y)$ to the initial correlation $C_0(t)=C_\Theta(X_0,Y_0)$ and of the instantaneous frequency $\omega(t)$ determined by Equation (4) to $\omega_0(t)$ reflects the quality of the inverse problem solution. The residual is taken as on the L_2-distance between the two functions:

$$r(C)=\frac{1}{W}\int\left(C(t)-C_0(t)\right)^2\mathrm{d}t \tag{10}$$

$$r(\omega)=\frac{1}{W}\int\left(\omega(t)-\omega_0(t)\right)^2\mathrm{d}t \tag{11}$$

W is the length of the time interval under study**.** The quality of the KM reconstruction is estimated through the relative residual given by Equations (10) and (11) normalized to the squared standard deviation:

$$r_0(C) = \frac{\int \left(C(t) - C_0(t)\right)^2 \mathrm{d}t}{\int \left(C_0(t) - \langle C_0(t)\rangle\right)^2 \mathrm{d}t} \tag{12}$$

$$r_0(\omega) = \frac{\int \left(\omega(t) - \omega_0(t)\right)^2 \mathrm{d}t}{\int \left(\omega_0(t) - \langle \omega_0(t)\rangle\right)^2 \mathrm{d}t} \tag{13}$$

3. A Specific Model and Illustrations

We will illustrate the inverse problem stated at the beginning of Section 2.3 with a specific model. Let us consider two series $X_0(t) = \sin\left(\theta_1(t)\right)$ and $Y_0(t) = \sin\left(\theta_2(t)\right)$ with $\theta_1(t)$ and $\theta_2(t)$ given by

$$\theta_1(t) = \int_0^t \frac{2\pi \,\mathrm{d}\tau}{(2\pi/\Omega) + a\sin(\Omega\tau/3)} + \frac{\pi t}{T}$$

$$\theta_2(t) = \int_0^t \frac{2\pi \,\mathrm{d}\tau}{(2\pi/\Omega) + a\sin(\Omega\tau/3)} - \frac{\pi t}{T}$$

with a = 0.9 year. When $\Theta = \frac{2\pi}{\Omega} \gg 1$ the two series $X_0(t)$ and $Y_0(t)$ oscillate with slowly varying frequency. When $T \gg \Theta$ the phase difference $\theta_1 - \theta_2$ is a slowly evolving function and the sliding correlation taken over time interval Θ may be estimated as:

$$C_0(t) = \cos(\theta_1 - \theta_2) = \cos\frac{2\pi t}{T}. \tag{14}$$

Their mean instantaneous frequency is:

$$\omega_0(t) = \frac{\dot{\theta}_1 + \dot{\theta}_2}{2} = \frac{2\pi}{2\pi/\Omega + a\sin(\Omega t/3)} = \frac{2\pi}{L_0(t)}.$$

And the mean instantaneous period is:

$$L_0(t) = \Theta + a\sin\left(\frac{\Omega t}{3}\right) \tag{15}$$

For this specific example we will perform two simulations with the Kuramoto model: one with non-symmetric coupling given by Equations (8) and (9) and one with the symmetric coupling given by Equation (8) and $\Delta\kappa(t) = 0$. Two quasi-periodic series $X(t) = \sin\left(\theta_1(t)\right)$ and $Y(t) = \sin\left(\theta_2(t)\right)$ are obtained from $\theta_1(t)$ and $\theta_2(t)$ whose evolution is given by the differential Equation (2) and the relevant coupling. The

reconstruction of the correlation will be compared for both cases, and the reconstruction of the instantaneous period will be described for the first case (Section 3.2).

3.1. Instantaneous Period and Frequency of Two Quasi-Periodic Series

In this section we describe how the instant frequency [$\omega(t)$] can be estimated from two quasi-periodic series $X(t)$ and $Y(t)$. First, we estimate individual instant periods $L_X(t)$ and $L_Y(t)$ for series $X(t)$ and $Y(t)$ respectively. Let $t_n^{\min}$ be times of minima and $t_n^{\max}$ be times of maxima of series $X(t)$. The value of the time difference between two successive minima $L_n = t_{n+1}^{\min} - t_n^{\min}$ is attributed to the time of the maximum $t_n^{\max}$ reached between the two minima $t_n^{\min}$ and $t_{n+1}^{\min}$. Thus we get a sequence of period lengths $(t_n^{\max}, L_n)$. Interpolating this sequence by cubic splines we obtain a continuous function of instantaneous period $L_X(t)$. The same procedure gives the $L_Y(t)$ function. The *combined instantaneous frequency* is defined as $\omega(t) = \frac{\omega_1(t) + \omega_2(t)}{2}$, where $\omega_1(t) = \frac{2\pi}{L_X(t)}$ and $\omega_2(t) = \frac{2\pi}{L_Y(t)}$.

3.2 Quality of the Reconstruction

Let us then consider the two series $X(t) = \sin(\theta_1(t))$ and $Y(t) = \sin(\theta_2(t))$ with $\theta_1(t)$ and $\theta_2(t)$ generated by Eq. (1) of the KM model with non-symmetric coupling. We assume that the correlation $C_0(t)$ and instantaneous period $L_0(t)$ are given by Equations (14) and (15) respectively and determine the coupling from Equations (8) and (9). The evolution of $X(t)$ and $Y(t)$ is presented on Figure 1a. Figure 1b shows the evolution of the instantaneous periods $L_X(t)$ and $L_Y(t)$ determined with the method described in Section 3.1 in comparison with

the instantaneous period $L_0(t)$ given be Equation (15). The individual instantaneous periods $L_X(t)$ and $L_Y(t)$ demonstrate oscillations similar to the oscillations of the instantaneous period $L_0(t)$ but have different amplitude (Figure 1b). Their amplitude varies because the varying correlation $C_0(t)$ given by Equation (14) influences the dissymmetry $\Delta\kappa(t)$ according to Equation (9). The *combined instantaneous period* $L(t)=\frac{2\pi}{\omega(t)}=\frac{\pi}{\omega_1(t)+\omega_2(t)}$ also follows the oscillations of $L_0(t)$ in frequency and phase but in contrast to individual series $L_X(t)$ and $L_Y(t)$ has constant amplitude independent of the correlation $C_0(t)$ (Figure 1c). Computing the closeness of the instantaneous period $L_0(t)$ with $L(t)$, $L_X(t)$ and $L_Y(t)$ we get $r_0=0.144$ and 0.146 for $L_X(t)$ and $L_Y(t)$ respectively and $r_0=0.065$ for $L(t)$. We conclude that the combined instantaneous period $L(t)$ better represents the real instantaneous period than the individual instantaneous periods $L_X(t)$ and $L_Y(t)$.

Figure 2 presents the Kuramoto reconstruction of correlation for the non-symmetric coupling (Figure 2a) and the symmetric coupling (Figure 2b). The correlation is well reproduced by KM in both cases (relative residuals are respectively 0.0017 and 0.000065). High-frequency noise on the correlation curve at Figure 2a is due to the influence of varying period on the estimation of the phase difference. Let us note that this inaccuracy in the reconstruction of correlation in the case of non-symmetric coupling is a fair price to pay for the possibility to reconstruct the instantaneous period. We lose in the quality of the reconstruction of the correlation (the relative residual is 0.0017 compared to 0.000065 in the symmetric case) and gain in the quality of the instantaneous period reconstruction (the relative residual is 0.065 compared to 1).

4. The Data

We now consider long series of solar proxies supposed to represent the toroidal and poloidal components of the solar magnetic field, namely the international sunspot number [R_I] and the aa-index.

4.1. Data Series

The daily values of R_I are provided without gaps from 1850 to the present by WDC-SILSO, Royal Observatory of Belgium, Brussels through sidc.oma.be/silso/ . The aa-index, introduced by Mayaud (1972), estimates the magnetic-disturbance level of the geomagnetic field within three-hour intervals based on the roughly antipodal observatories of Greenwich and Melbourne and their successors. We use the daily values provided from 1868 to now by the International Service of Geomagnetic Indices (ISGI) via isgi.latmos.ipsl.fr/source/indices/aa/**.** In order to smooth these daily series we take their one-year sliding average with a daily sampling. The evolution of resulting indices R_I and aa is presented in Figure 3. As in (Blanter *et al.* 2014) we compute the correlation $C_0(t)$ between R_I and aa-index over an 11-year sliding window centered at time t with one day sampling.

4.2. The Instantaneous Period of the Solar Cycle

Inspired by the model results of the previous section, we start from two quasi-periodic series R_I and aa, and we construct relevant series of instantaneous periods, $L_{RI}(t)$ and $L_{aa}(t)$, respectively; relevant frequencies $\omega_{RI}(t)=\frac{2\pi}{L_{RI}(t)}$ and $\omega_{aa}(t)=\frac{2\pi}{L_{aa}(t)}$; combined instantaneous frequency $\omega_0(t)=\frac{\omega_{RI}(t)+\omega_{aa}(t)}{2}$, and combined instantaneous period $L_0(t)=\frac{2\pi}{\omega_0(t)}$. Difficulties appear at the first step of this construction: whereas we can easily locate minima and maxima in the simulated series of Figure 1a, it can be a tricky task for real solar proxies, especially for the aa-index (Figure 3). In order to avoid taking a local minimum of the index reached during a period of maximal activity as a minimum of the cycle

(e.g. the local minimum of the aa-index in 1884), we follow the rule that the distance from the true minimum to the next maximum [$d_r = t_n^{\max} - t_n^{\min}$] should be longer than the minimal observed rise time, and the minimal distance from the maximum to the next minimum [$d_f = t_{n+1}^{\min} - t_n^{\max}$] should be longer than the minimal observed falling time. Values of observed rising and falling stages of solar cycle are available from NGDC via ftp://ftp.ngdc.noaa.gov/STP/space-weather/solar-data/solar-indices/sunspot-numbers/cycle-data/table_cycle-dates_maximum-minimum.txt and given in Table 1. Thus we determine the minimum [$t_{n+1}^{\min}$] as the absolute minimum of the index reached in the interval $[t_n^{\max} + f_{\min}, t_n^{\max} + f_{\max}]$, where $f_{\min}$ and $f_{\max}$ denote the minimal and the maximal lengths of the falling stage of the solar cycle given in Table 1. Similarly, the next maximum [$t_n^{\max}$] is determined as the absolute maximum of the index reached on the interval $[t_n^{\min} + r_{\min}, t_n^{\min} + r_{\max}]$, where $r_{\min}$ and $r_{\max}$ denote the minimal and the maximal lengths of the rising interval of the solar cycle given in Table 1. Values of minima and maxima determined for the R_I and aa-series are used to obtain the two series of instantaneous period $L_{RI}(t)$ and $L_{aa}(t)$ with the interpolation procedure described in Section 3.1. The resulting curves of the instantaneous periods are presented in Figure 4.

Let us note that the interpolation used in the construction of instantaneous period curve may be applied only inside the time interval $\left[t_1^{\max}, t_N^{\max}\right]$ where $t_1^{\min} < t_1^{\max} < ... < t_N^{\max} < t_{N+1}^{\min}$, and therefore we lose the time intervals outside this interval. The interpolation also deforms the first and last cycles on the model curve (Figure 1c), which also should be taken into account as a possible edge effect.

5. Application of the Kuramoto Model to Solar Indices

We now apply the Kuramoto model described by Equation (1) to the inverse problem of the reconstruction of the 11-year sliding correlation

$C_0(t) = C_\Theta(R_\mathrm{I}, \mathrm{aa})$ ($\Theta = 11$ years) and the mean instantaneous frequency $\omega_0(t) = \frac{\omega_{\mathrm{RI}}(t) + \omega_{\mathrm{aa}}(t)}{2}$. The procedure of the Kuramoto model reconstruction (KMR) is similar to the procedure described by Blanter et al. (2014), except that here we need to determine the mean coupling [$\kappa(t)$] and its dissymmetry [$\Delta\kappa(t)$]. Equations (3)–(5) allow us to determine them independently. The determination of the mean coupling does not differ from the determination of coupling in the Kuramoto model with symmetric coupling and we therefore can use the results obtained by Blanter et al. (2014).

5.1. Mean Coupling

To get the mean coupling $\kappa(t)$ we express $\theta_0(t)$ through the correlation $C_0(t)$ by Equation (6) and substitute it in Equation (5), obtaining two solutions:

$$\theta_0(t) = \arccos\left(C_0(t)\right)$$
$$\kappa(t) = \frac{2\Delta\omega - \left(\arccos\left(C_0(t)\right)\right)'}{\sin\left(\arccos\left(C_0(t)\right)\right)}, \text{ for } C_0(t) > 0$$

(15)

$$\theta_0(t) = -\arccos\left(C_0(t)\right)$$
$$\kappa(t) = \frac{-2\Delta\omega - \left(\arccos\left(C_0(t)\right)\right)'}{\sin\left(\arccos\left(C_0(t)\right)\right)}, \text{ for } C_0(t) < 0$$

A change of a branch of solution in Equation (15) corresponds to the change of the leading oscillator.

The possibility of a synchronization between the two oscillators in Equation (1) depends on the strength of the mean coupling [$\kappa(t)$] relative to the value of the parameter $\Delta\omega$; one must have:

$$\kappa^2(t) > 4\Delta\omega^2. \quad (16)$$

Equation (16) imposes restrictions on the variability of correlation $C_0(t)$:

$$\left(\left(\arccos\left(C_0(t)\right)\right)'\right)^2 < 4\Delta\omega^2 \quad (17)$$

Expression (17) means that if we chose parameter $\Delta\omega$ to be reasonably large and the daily variation of the correlation between R_I and aa is reasonably small, then the KM reconstruction is possible (see Blanter *et al*, 2014). Evolution of the mean coupling $[\kappa(t)]$ for two values of the frequency difference, $\Delta\omega = 0.5$ and $\Delta\omega = 0.2$, is presented in Figure 5a ($\Omega = \frac{2\pi}{11}\,\mathrm{y}^{-1}$).

5.2. Coupling dissymmetry

We take the combined instantaneous frequency $\omega_0(t) = \frac{\omega_{\mathrm{RI}}(t) + \omega_{\mathrm{aa}}(t)}{2}$ and substitute it in the first of Equations (3). The coupling dissymmetry $[\Delta\kappa(t)]$ is

$$\Delta\kappa(t) = \frac{2\left(\Omega - \omega_0(t)\right)}{\sin\left(\theta(t)\right)} \tag{18}$$

Let us note that when the correlation $[C_0(t)]$ changes from positive to negative, this change corresponds to a change in the order of the two differential equations in Equation (2). The sign of the phase difference $[\theta(t)]$ changes simultaneously with the sign of the coupling dissymmetry contribution to the right side term of Equation (2). Consequently the coupling dissymmetry $[\Delta\kappa(t)]$ does not depend on the sign of the correlation and can be obtained from Equation (9). The evolution of $\Delta\kappa(t)$ is presented in Figure 5b; according to Equation (9) it does not depend on $\Delta\omega$.

5.3. Kuramoto Model Reconstruction (KMR)

Now we consider the inverse problem of reconstruction of the correlation and instantaneous period with synthetic series simulated by the Kuramoto model. We use the mean coupling $[\kappa(t)]$ and its dissymmetry $[\Delta\kappa(t)]$ estimated by Equations (8) and (9) to obtain the evolution of simulated phases $\theta_1(t)$ and $\theta_2(t)$ satisfying Equation (1). Two synthetic

series [$X(t)=\sin(\theta_1(t))$ and $Y(t)=\sin(\theta_2(t))$] are generated by the Kuramoto model. Their sliding correlation [$C(t)=C_\Theta(X,Y)$] computed with a daily sampling over the interval $\Theta=\frac{2\pi}{\Omega}$ centered at day t is compared with $C_0(t)=C_\Theta(R_I,\mathrm{aa})$ (Figure 5c). The combined instantaneous period $L(t)=\frac{2\pi}{\omega(t)}=\frac{\pi}{\omega_X(t)+\omega_Y(t)}$ interpolated from series $X(t)$ and $Y(t)$ by the method described in Section 4.1 is compared with $L_0(t)=\frac{2\pi}{\omega_0(t)}=\frac{\pi}{\omega_{RI}(t)+\omega_{aa}(t)}$ (Figure 5d). The quality of the reconstructions is evaluated by the relative residuals, which takes the values $r_0(C)=0.13$ and $r_0(L)=0.15$.

5.4. Effect of Preliminary Averaging

In the previous section we considered the annual running means of solar indices. Let us now check the effect of the length of the window [***V***] of preliminary averaging on the quality of the KMR. Comparing original data series smoothed by averaging over one, two, and four-year-long sliding window, we see that the shape and positions of minima and maxima of the R_I series are rather stable (Figure 6a); they are somewhat less stable in the case of the aa-index (Figure 6b). In spite of the sensitivity of the aa-index to preliminary averaging, the correlation $C(R_I,\mathrm{aa})$ computed over 11-year running window has the same shape for all windows [*V*] (Figure 6c). On the other hand, the length of the combined instantaneous period for *V*=1 year disagrees with the combined instantaneous periods for *V*=2 and 4 years (Figure 6d).

Table 2 presents the quality of the KMR reconstruction when different windows of preliminary averaging are used to compute the sliding correlation and the instantaneous period curves of R_I and aa-indices. The correlation is reconstructed with the same quality for each averaging in contrast to the instantaneous period, for which the reconstruction is better for *V*=2 and 4 years than for *V*=1 year. From Table 2 and Figure 6, we suggest that preliminary averaging of the aa-index should be longer than

one year. When the one-year averaging of the aa-index is considered, the high-frequency noise distorts the true evolution of the length of the cycle. Let us note that the evolutions of the combined instantaneous periods for V=2 and 4 years are similar but do not follow the evolution of the combined instantaneous period for V=1 year (Figure 7a–c). They are also similar to the evolution of the R_I instantaneous period which is less dependent on the preliminary averaging than for the aa-index (Figure 7d–f).

5.5. Toroidal and Poloidal Components of the Solar Magnetic Field.

Let us now replace the aa-index by the index aa_p considered as a better proxy of the poloidal component of the solar magnetic field. The aa_p-index is defined by removing from the aa-index the part that depends linearly on R_I (Ruzmaikin and Feynman, 2001):

$$aa_P(t) = aa(t) - 0.07R_I(t) - 5.17 \qquad (19)$$

The sunspot number index [R_I] is again considered to be representative of the toroidal component. We perform the same simulation as above for the two series R_I and aa_p and present the results of KM reconstruction in Figure 8. The quality of this reconstruction is characterized by the values $r_0(C) = 0.077$ and $r_0(L) = 0.123$.

Two interesting features appear in Figure 8. First, a change of the sign of the correlation happens in 1925; by construction, the KM reconstructs only the low-frequency component of the evolution of correlation and allows separating it from the high-frequency variations. On the plot of reconstructed correlation (Figure 8b, red curve) the sign reversal is evident. For the two non-linear oscillators this reversal means a change of leading oscillator. The second feature consists in the remarkable regularity of the variations of the combined instantaneous period of R_I and aa_p-indices and its reconstruction (Figure 8d). We observe a clear periodicity of about 30–33 years. These variations are similar to the variations of the combined instantaneous period of R_I and aa obtained at V=4 years (Figure 7c).

5.6 Effect of De-Correlation on the Reconstruction of the Instantaneous Period

In contrast to the high correlation between R_I and aa at the beginning of the graph (Figure 5c), the corresponding correlation between R_I and aa_p is close to zero (Figure 8b). As a result, the simulated series [*X* and *Y*] have an irregular behavior at the beginning of the time span under consideration (Figure 9a). Therefore, the edge effect that bears on the estimation of the combined instantaneous period estimation of the *X* and *Y* series is stronger (Figure 9b) and the departure from the combined instantaneous period of the real series R_I and aa_p is longer than in the previous simulations (compare Figure 9b with Figures 5d, 7a–c). The corresponding relative residual $r_0(L) = 0.308$ is twice as large as the values in Table 2. This discrepancy disappears if we start the simulation at any time when high values of correlation $C_0(R_I, aa_P)$ are observed. We attribute this irregularity of the reconstruction to the local de-synchronization effect linked to the weak coupling: according to Equation (8) low values of correlation $C_0(t)$ together with relatively high values of the derivative $(\arccos C_0(t))'$ lead to weak coupling and produce an irregularity in the simulated series. The combined instantaneous period (Figure 9b) is evidently more sensitive to such irregularity than the correlation (Figure 8b).

6. Discussion and Conclusions

We have attempted to represent the interactions between the toroidal and poloidal components of the solar magnetic field as a coupling between two non-linear Kuramoto oscillators. Variations of solar-cycle length appear in the Kuramoto model as a result of a dissymmetry of the coupling. We note that, in terms of a solar dynamo, the dissymmetry between the generation of poloidal and toroidal magnetic fields seems to be a more realistic assumption than the symmetric coupling considered by Blanter et al. (2014): the relative dissymmetry ($\Delta\kappa/\kappa \approx 0.1$ to 0.2) between the coupling coefficients generates deviations of cycle length from its mean value. The evolution of the cycle length follows the evolution of the

coupling dissymmetry when the system is well synchronized, but it becomes unstable in periods of de-synchronization (*e.g.* time intervals of low absolute values of correlation between the aa and R_I indices). Solar Cycle 21 is a recent example of such a de-synchronization. This may be an explanation why Cycle 21 does not obey the Waldmeier statistical relations between solar cycle rise time and amplitude (*e.g.* Kane, 2008).

6.1. Amplitude Variations

It is well-known that solar cycle amplitude varies from cycle to cycle. Our model does not reconstruct these amplitude variations; yet, the neglected amplitude may influence variations of solar cycle length and the quality of the combined instantaneous period KMR. We have performed complementary simulations that show that the contribution of the high-frequency amplitude variations is small and do not degrade the quality of KMR (see Section A2 of the Appendix). On the contrary, slow variations of the cycle amplitude are important both for variations of the instantaneous period and KMR quality (see Section A3 of the Appendix). However, amplitude variations cannot explain the whole range of the observed variations in solar-cycle length (Section A3). The model example presented in the Appendix gives an upper bound for the amplitude contribution, because the actual difference of the amplitude between any two actual consecutive solar cycles is smaller than the difference reached in the model. Contrary to most model simulations which produce better quality of the KMR than that we see for solar indices, the model with a slow amplitude variation gives KMR relative residuals that are two times larger. We come to the natural conclusion that a Kuramoto model reconstructs the combined instantaneous period variations better when they originate from a variation of actual frequency than from a variation of amplitude (see Figure 7, Section 3.2 and Appendix). The good quality obtained in the KMR of the combined instantaneous period of the solar cycle (Figure 7) indicates that the main part of the solar-cycle period variations indeed comes from a frequency variation and not from an amplitude variation.

6.2 “Three Cycle” Quasi Periodicity

The “best” reconstruction of the solar instantaneous period at four year averaging from the R_I and aa series and that based on R_I and aa_p series shows a similar modulation of the solar cycle length with characteristic

times of 30–35 year. There are other findings of 30–40 year periodicities obtained by harmonic analysis in the amplitude characteristics of solar activity (*e.g.* Duhau and Chen, 2002; Kane, 2007; Richards, Rogers, Richards, 2009). However the significance of these periods is debated. On one hand, the power at these periods in the wavelet spectrum is not large and results based on data with different sampling rates are so contradictory that some authors do not accept the existence of any significant periodicity between the Hale and Gleissberg cycles (*e.g.* Solheim, 2013). On another hand, a recent wavelet analysis of SSN and aa performed by Singh and Badruddin (2014) at three different temporal resolutions (daily, monthly and yearly) reveals 95 % significant periodicities of 30–32 year in the aa-index and 36–38 year in sunspot numbers (SSN); a "three-cycle" quasi-periodicity was also reported in cosmic ray data (Ahluwalia, 2012; Perez-Peraza *et al.* 2012). This range of solar periodicity attracts special attention because similar periods are found in the monsoon rainfall data (Agnihotri *et al.* 2002) and may be considered as evidence in favor of a widely investigated relationship between solar activity and Earth climate (*e.g.* Cliver, Borikoff, Feyman, 1998; de Jager, Duhau, van Geel, 2010; Lockwood, 2012). We suggest that the 30–35 years modulation of solar-cycle length found in the present paper may be responsible for the sporadic appearance of the "three-cycle" quasi-periodicity in different solar indices, due to the Waldmeier effect which proposes a link between the amplitude and the length of solar cycle (Solanki *et al.* 2002).

6.3 Quasi-Biennial Oscillations

The Kuramoto model reconstructs only low-frequency variations of the solar-cycle length and phase. However strong high-frequency variations in solar activity are present and they affect the quality of the reconstruction. Despite preliminary averaging of data that effectively attenuates variations with characteristic times less than one year we see that the evolution of the solar-cycle length visibly changes when we pass from one- to two- or four-year sliding averaging (Figure 6); the quality of the solar-cycle length reconstruction is better when it is estimated for series preliminary averaged over V=2 or 4 year rather than for V=1 year (Table 2). The solar cycle length series estimated for sunspot number [R_I]

and relevant to one-, two- and four-year of preliminary averaging correlate with coefficients 0.89, 0.93, and 0.97 respectively (Table 3). In contrast to sunspot number, the aa-index solar cycle length estimated at one year averaging anti-correlates with the same series estimated at two- and four-year averaging; it also anti-correlates with the cycle length series estimated for R_I (Table 3). We attribute this discrepancy to a contribution of medium range periodicities, such as the quasi-biennial oscillations (*e.g.* Mursula, Zieger, Vilpolla, 2003; Bazilevskaya *et al.* 2014) and by the 3.5–3.8 year periodicities found in the evolution of active regions (Berdyugina and Usoskin, 2003). These periodicities are not reduced by one-year averaging and they affect the definition of minima and maxima of solar activity resulting in variability of the solar-cycle length. Let us note that the correlation between indices is not affected by the quasi-biennial oscillations: therefore the phase shift is always reconstructed with the same quality (Table 3). We conclude that quasi-biennial oscillations affect the determination of the solar-cycle period in the aa-index but do not affect its long-term correlation with sunspot number.

6.4. Solar Dynamo

We consider the sunspot number [R_I] and the aa-index to be relevant proxies of the toroidal and poloidal components of the solar magnetic field respectively and suggest that the evolution of couplings [κ_1 and κ_2] represents that of interactions between the toroidal and poloidal parts of the solar magnetic field. Couplings κ_1 and κ_2 may be considered as a global representation of the physical processes responsible for the generation of poloidal and toroidal solar magnetic field, schematically representing the concepts behind αΩ-dynamos. The dissymmetry of the two couplings naturally induces variability in solar cycle duration. Let us note that when one changes one of the two couplings, their difference changes, affecting the dissymmetry and contributing to the variability of the solar cycle length. Most processes known to affect the length of the solar cycle such as fluctuations of the poloidal field generation or variations of the meridional flow (Karak *et al.* 2014) affect the generation of only one component of the solar magnetic field. Consequently they

influence only one coupling and change the dissymmetry. Let us note that the dissymmetry of couplings affects the true frequency of the mean solar cycle, which may be different from the solar-cycle length estimated uniquely from the toroidal magnetic field component.

There is no direct observation of solar dynamo processes within the solar interior, and most surface observations of the solar magnetic field have only short records. Using available long but indirect surface data we combine solar dynamo processes with their image on the solar surface. For example, the lack of sunspots during periods of Grand Minima (*e.g.* Maunder or Dalton minima) does not imply the disappearance of the solar cycle even though uncertainties in estimates of its length become greater than usual (*e.g.* Usoskin and Mursula, 2003; Richards, Rogers, Richards 2009; Usoskin, 2013). The physical interpretation of the change in coupling is therefore a difficult task that requires further investigation. Other indices, such as observations of sunspot areas, tilt angle, or polar faculae can be used as proxies of the toroidal and poloidal components instead of R_I and aa-indices (see *e.g.* Miñoz-Jaramillo *et al.* 2013). Different filtering and temporal resolutions should allow to distinguish a stable long-term evolution of the coupling from random features and interpret it in terms of the solar dynamo.

6.5. Solar-Cycle Length Definition

Several attempts have been made to use solar-cycle length to predict the amplitude of the next solar cycle, as a follow up of the Waldmeier relationship (*e.g.* Kane 2008; Vaquero and Trigo, 2008). There are different estimates of the solar-cycle length (*e.g.* Fligge, Solanki, Beer, 1999; Solanki *et al.* 2002; Usoskin and Mursula, 2003); however they usually treat only one series (*e.g.* sunspot number or sunspot-group number). The Kuramoto model shows that the cycle length estimated from only one index is more affected by the variation of the strength of correlation between indices than the combined period length estimated from both indices R_I and aa (Figure 1). This sensitivity of the sunspot-number cycle length to the evolving correlation may lead to an instability in the solar-amplitude prediction (*e.g.* Kane, 2008). We note that the 30–35 year periodicity in the length of solar cycle appears in the mean period

length $L(t) = \frac{L_{RI} + L_{aa}}{2}$, but it is less pronounced in the sunspot number cycle length series L_{RI} (Figure 7f). However our records of solar indices are too short to propose a definite statement about the origin or significance of the 30–35-year modulation of the solar-cycle length.

Acknowledgements: We thank the anonymous reviewer for very constructive comments that helped improve the manuscript significantly. This is IPGP contribution no 3713.

Disclosure of Potential Conflict of Interest: authors declare that they have no conflicts of interest.

References

Acebron, J.A., Bonilla, L.L., Vicente C.J.P., Ritort, F.: 2005, *Rev. Mod/ Phys.* **77**, 137.doi: 10.1103/RevModPhys.77.137

Ahluwalia, H.S.: 2012, *Indian J. Radio Space Phys*. **41**, 509.

Agnihotri, R., Dutta, K., Bhushan, R., Somayajulu, B.L.K.: 2002. *Earth Planet. Sci. Lett.* **198**, 521.doi: 10.1016/S0012-821X(02)00530-7

Ashwin, P. Burylko, O. and Maistrenko, Y.: 2008. *Phys. D: Non. Phe.*, **237**, 454. doi: 10.1016/j.physd.2007.09.015

Bazilevskaya, G., Broomhall, A.-M., Elsworth, Y., Nakariakov, V.M.: 2014, *Space Sci. Rev*. **186**, 359. doi: 10.1007/s11214-014-0068-0

Blanter, E., Le Mouel, J.-L., Shnirman, M., Courtillot, C.: 2014. *Solar Phys*. **289**, 4309. doi : 10.1007/s11207-014-0568-9

Charbonneau, P.: 2010. *Living Rev. Solar Phys.* **7**, 3.doi:10.12942/lrsp-2010-3

Cliver, E.W., Borikoff, V., Feynman, J.: 1998. *Geophys. Res. Lett.* **25**, 1035. doi: 10.1029/98GL00499

Cumin, D., Unsworth, C.P.: 2007, *Physica D: Nonlinear Phenomena*, **226**, 181.doi: 10.1016/j.physd.2006.12.004

De Jager, C., Duhau, S., van Geel, B.: 2010, *J. Atmos. Solar-Terr. Phys.* **72**, 926.doi: 10.1016/j.jastp.2010.04.011

Dorfler, F., Bullo, F.: 2011, *SIAM J. on Applied Dynamical Systems*, **10**, 1070. doi: 10.1137/110851584

Dorfler, F., Bullo, F.: 2014, *Automatica*, **50**, 1539.doi: 10.1016/j.automatica.2014.04.012

Duhau, S., Chen, C.Y.: 2002, *Geophys. Res. Lett.* **29**, 1628. doi: 10.1029/2001GL013953

Fligge, M., Solanki, S.K., Beer, J.: 1999, *Astron. Astrophys*., **346**, 313

Hathaway, D.H.: 2015. *Living Rev. Solar Phys.* **12**, 1.doi: 10.1007/lrsp-2015-4

Hazra, G., Karak, B.B., Banerjee, D., Choudhuri, A.R.: 2015, *Solar Phys*. **290**, 1851.doi: 10.1007/s11207-015-0718-8

Kane, R.P.: 2007, *Solar Phys.*, **246**, 487. doi: 10.1007/s11207-007-9059-6

Kane, R.P.: 2008, *Solar Phys.* **248**, 203. doi: 10.1007/s11207-008-9125-8

Karak, B.B., Jiang, J., Miesch, M.S., Charbonneau, P., Choudhuri, A.R.: 2014, *Space Sci. Rev.* **186**, 561. doi: 10.1007/s11214-014-0099-6

Lockwood, M.: 2012, *Surveys in Geophysics*, **33**, 503, doi: 10.1007/s10712-012-9181-3

Lopes, I., Passos, D., Nagy, M., Petrovay, K.: 2014, *Space Sci. Rev.* **186**, 534.doi: 10.1007/s11214-014-0066-2

Mayaud, P.N.: 1972, *J. Geophys. Res.* **77**, 6870. doi : 10.1029/JA077i034p06870

Muñoz-Jaramillo, A., Dasi-Espuig, M., Balmaceda, L.A., DeLuca E.E.: 2013, *Astrophys. J.* **767**, L25, doi: 10.1088/2041-8205/767/2/L25

Mursula, K, Zieger, B., Vilppola, J.H.: 2003, *Solar Phys.* **212,** 201. doi: 10.1023/A:1022980029618

Nagy, M., Petrovay, K.: 2006, *Astron. Nachr*. **999**, 789.

Passos, D. and Lopes, I.: 2008. *Solar Phys.* **250**, 403. doi: 10.1007/s11207-008-9218-4

Perez-Peraza, J., Velasco, V., Libin, I.Y., Yudakhin, K.F.: 2012. *Adv. Astron.* **1**. doi: 10.1155/2012/691408

Popovych, O.V., Maistrenko, Y.L., Tass, P.A.: 2005, *Phys. Rev. E* **, 71**, 065201. doi: 10.1103/PhysRevE.71.065201

Richards, M., Rogers, M., and Richards, D.: 2009, *Publ. Astron. So. Pac.* **121**, 797. doi: 10.1086/604667

Ruzmaikin, A., Feynman, J.: 2001, *J. Geophys. Res.* **106**, 15783. doi: 10.1029/2000JA000287

Singh, Y.P., Badruddin: 2014, *Planet. Space Sci.* **96**, 120. doi: 10.1016/j.pss.2014.03.019

Solanki, S.K., Krivova, N.A., Schüssler, M., Fligge, M.: 2002, *Astron. Astrophys.* **396**, 1029. Doi: 10.1051/0004-6361:20021436

Solheim, J.-E.: 2013, *Pattern Recogn. Phys.* **1**, 159. doi: 10.5194/prp-1-159-2013

Strogatz, S.H.: 2000, *Physica D* **143**, 1. 10.1016/S0167-2789(00)00094-4

Svalgaard, L., Cliver, E.W.: 2007, *Adv. Space Res.***40**, 1112. doi: 10.1016/j.asr.2007.06.066

Tilles, P.F.C., Cerdeira, H.A., Ferreira, F.F: 2013, *Chaos, Solitons And Fractals*, **49**, 32. doi: 10.1016/j.chaos.2013.02.008

Usoskin, I.G.: 2013, *Living Rev. Sol. Phys.* **10**, 1, doi: 10.12942/lrsp-2013-1

Usoskin, I. G., Mursula, K.: 2003, *Solar Phys*. **218**, 319. doi : 10.1023/B:SOLA.0000013049.27106.07

Vaquero, J.M., and Trigo, R.M.: 2008, *Solar Phys.* **250**, 199. doi : 10.1007/s11207-008-9211-y

Vieira, L.E.A., Solanki, S.K.: 2010, *Astron. Astrophys.* **509**, A100. doi: 10.1051/0004-6361/200913276

Appendix. Variation of the Combined Instantaneous Period Produced by Amplitude Variations.

In the main part of the article, we focus on the frequency evolution and neglect the influence of solar-cycle amplitude on the estimate of its length. In this appendix, we consider several hypotheses concerning solar cycle amplitude and its effect on the estimate of the solar cycle combined instantaneous period and on its reconstruction by a Kuramoto model. For this purpose, we consider two synthetic series $X_0(t) = a + A(t)\sin(\Omega t + \varphi(t))$ and $Y_0(t) = a + A(t)\sin(\Omega t - \varphi(t))$ and investigate how the evolution of the amplitude, [$A(t)$], affects the evolution of the combined instantaneous period $L_0(t) = \frac{2\pi}{\omega_0(t)}$, where the combined instantaneous frequency is estimated according to the method described in Section 3.1. When the combined instantaneous period [$L_0(t)$] is clearly affected by the amplitude, we perform a KMR and evaluate the reconstruction quality. Two series $X(t)$ and $Y(t)$ are generated by the Kuramoto model as described in Section 2.3. The relevant mean coupling and its dissymmetry are given by Equations (8) and (9) respectively, in which we substitute the combined instantaneous frequency [$\omega_0(t)$] and the correlation $C_0(t) = C(X_0(t), Y_0(t))$.

A1. Quasi-Constant Amplitude

When the amplitude of the solar cycle is assumed to be constant within each solar cycle and changes in a step-like fashion between two consecutive cycles, this variation does not affect (by construction) the combined instantaneous period. In our simulations, we use a smooth connection between two consecutive cycles at the minimum point.

A2. High-Frequency Noise in the Amplitude

When the amplitude [$A(t)$] is taken as a series of independent random values [$A_{\min} < A(t_n) < A_{\max}$], the correlation $C_0(t) = C\left(X_0(t), Y_0(t)\right)$ should be corrected with respect to $\cos\left(2\varphi(t)\right)$ by a factor depending on the mean value [A_0] and on the standard deviation [σ] of its distribution, as follows:

$$C_0(t) == \frac{\cos\left(2\varphi(t)\right)}{\left(1+\frac{\sigma^2}{A_0^2}\right)^2} . \qquad (20)$$

The more general expression of the correction factor when parameters of the noise are different for the series X_0 and Y_0 and relevant demonstrations may be found in (Blanter *et al.* 2014). Let us note that when we perform a one-year preliminary averaging, we strongly reduce the standard deviation [σ] and make the noise Gaussian.

The evolution of the instantaneous period variation of the individual series $L_X(t)$ and $L_Y(t)$ follows the evolution of the phase difference [$2\varphi(t)$] (Figure 10). The variation of the combined instantaneous period induced by any reasonable noise is small compared to the variation observed in the solar cycle. For example, if the amplitude is uniformly distributed within an interval $[A_0 - 1, A_0 + 1]$ and the frequency Ω is equal to $2\pi/11$ year^{-1} we obtain variation of the combined instantaneous period to be less than 0.25 year (Figure 10, top panel, dashed red curve). When an annual preliminary averaging is applied to the two X_0 and Y_0 series, the period variation falls to 0.13 year (Figure 11, top panel, dotted-red curve). This is over one order of magnitude less than the 1.5-year amplitude of the variation of the combined instantaneous period of the R_I and aa-series (Figure 4), which is estimated in the same way. We conclude that a high-frequency noise cannot significantly affect the combined instantaneous period variation.

A3. Slowly Oscillating Amplitude

When the amplitude [$A(t)$] slowly evolves with time, it does affect the variation of the combined instantaneous period. As an example, we consider an amplitude evolving as $A(t)=4+2\sin(\nu t)$ with frequency [ν] corresponding to a 25 year period of oscillation $\nu=\frac{2\pi}{25}$ y^{-1}. Two synthetic series $X_0(t)=a+A(t)\sin(\Omega t+\varphi(t))$ and $Y_0(t)=a+A(t)\sin(\Omega t-\varphi(t))$ with parameters $a=6$, $\Omega=\frac{2\pi}{11}y^{-1}$, $\varphi(t)=1-\cos(\gamma t)$, and $\gamma=\frac{2\pi}{66}y^{-1}$ are presented in Figure 10,a. The ratio between the amplitudes of two cycles in the synthetic series (Figure 11, top) is larger than the ratio between the amplitudes of the yearly averaged R_I or aa -series (Figure 3). The variation of the combined instantaneous period oscillates with the same 25-yest period as the amplitude (Figure 11, bottom), but the amplitude of these oscillations is about 0.75 year, which is two times less than the 1.5-year in solar indices.

Let us now consider the quality of the instantaneous period reconstruction by the Kuramoto model. The relative residual of the $L_X(t)$ and $L_Y(t)$ reconstructions are 0.02 and 0.018 respectively, which is comparable to or much better than relevant residuals of the $L_{RI}(t)$ and $L_{aa}(t)$ reconstructions. On the contrary, the relative residual of the combined instantaneous period is equal to $r_0(L)$=0.37 which is two times larger than the relative residuals of the combined instantaneous period of R_I and aa-indices (Table 2). We conclude that although the main results were obtained in this article disregarding amplitude changes in the solar cycle they cannot be explained by amplitude variations and that the KMR with non-symmetrical couplings robustly reconstructs variations in solar-cycle length.

Table 1. Solar Cycle data including dates of minima and maxima, rise, fall and cycle lengths.

Sunspot cycle number [n]	Year of Min [$T_n^{\min}$]	Year of Max [$T_n^{\max}$]	Rise to Max (y) [r]	Fall to Min (y) [f]	Cycle Length (y) [L_n]
1	1755.2	1761.5	6.3	5.0	11.3
2	1766.5	1769.7	3.2	5.8	9.0
3	1775.5	1778.4	2.9	6.3	9.2
4	1784.7	1788.1	3.4	10.2	13.6
5	1798.3	1805.2	6.9	5.4	12.3
6	1810.6	1816.4	5.8	6.9	12.7
7	1823.3	1829.9	6.6	4.0	10.6
8	1833.9	1837.2	3.3	6.3	9.6
9	1843.5	1848.1	4.6	7.9	12.5
10	1856.0	1860.1	4.1	7.1	11.2
11	1867.2	1870.6	3.4	8.3	11.7
12	1878.9	1883.9	5.0	5.7	10.7
13	1889.6	1894.1	4.5	7.6	12.1
14	1901.7	1907.0	5.3	6.6	11.9
15	1913.6	1917.6	4.0	6.0	10.0
16	1923.6	1928.4	4.8	5.4	10.2
17	1933.8	1937.4	3.6	6.8	10.4
18	1944.2	1947.5	3.3	6.8	10.1
19	1954.3	1957.9	3.6	7.0	10.6
20	1964.9	1968.9	4.0	7.6	11.6
21	1976.5	1979.9	3.4	6.9	10.3
22	1986.8	1989.6	2.8	5.3	10.0
23	1996.9	2000.3	3.5	8.6	12.2
24	2008.9				

Table 2. Qualities of the KMR for R_I and aa-series depending on the window W (in years) of preliminary averaging.

	W	Correlation					
		1		2		4	
		r_0(C)	r_0(L)	r_0(C)	r_0(L)	r_0(C)	r_0(L)
Instantaneous period	1	0.128	0.171	0.127	0.161	0.132	0.154
	2	0.140	0.085	0.147	0.100	0.163	0.185
	4	0.137	0.058	0.142	0.074	0.157	0.156

Table 3. Correlation coefficients between solar-cycle length series estimated for R_I and aa-indices after one-, two- or four-years sliding averaging.

W [years]	$C(L_{RI}, L_{aa})$	aa-index			R_I-index		
		1	2	4	1	2	4
1	-0.35	1	-0.68	-0.62	1	0.89	0.97
2	0.49		1	0.79		1	0.93
4	0.67			1			1

Figure captions:

Figure 1. Reconstruction of the instantaneous period. **(**a): two synthetic series simulated by the Kuramoto model $X(t)$ (dotted-blue) and $Y(t)$ (solid-red). (b): instantaneous period $L_0(t)$ used for modeling (dashed-green curve) and instantaneous periods $L_X(t)$ (dotted-blue) and $L_Y(t)$ (solid-red) estimated from series $X(t)$ and $Y(t)$ by the way described in Section 3.1 and 4. (c): instantaneous period $L_0(t)$ (dotted-green curve) and the cumulative instantaneous period of model series $L(t)$ (solid-magenta). Parameters of simulation are: T=240y, $\Theta = \frac{2\pi}{\Omega} = 11\,\mathrm{y}$, $\Delta\omega = 0.5$.

Figure 2. Reconstruction of sliding correlation by the Kuramoto model with non-symmetric (a) and symmetric (b) coupling. Initial curves of correlation (blue) are compared with KM reconstruction (red). Equations for the sliding correlation and instantaneous frequency: see main text. Parameters of simulation are: $T = 240\,\mathrm{y}$, $\Theta = \frac{2\pi}{\Omega} = 11\,\mathrm{y}$, $\Delta\omega = 0.5$.

Figure 3. Evolution of sliding annual means of solar indices R_I (dotted-blue) and aa (multiplied by 10, solid-red).

Figure 4. Evolution of instantaneous periods of solar activity: $L_{\mathrm{RI}}(t)$ (dotted-blue), $L_{\mathrm{aa}}(t)$ (dashed-green) and their combined instantaneous period $L_0(t)$ (solid-red).

Figure 5. Kuramoto model simulation performed for R_I and aa-indices. (a) – mean coupling $\kappa(t)$ for $\Delta\omega = 0.5$ (red) and $\Delta\omega = 0.2$ (thin-green); (b) – coupling dissymmetry $\Delta\kappa(t)$; (c) – evolution of correlation $C_0(t) = C(R_\mathrm{I}, \mathrm{aa})$ (dotted-blue) and its KMR $C(t) = C(X, Y)$ (solid-red); (d) – evolution of combined instantaneous period $L_0(t) = \frac{2\pi}{\omega_0(t)} = \frac{\pi}{\omega_{\mathrm{RI}}(t) + \omega_{\mathrm{aa}}(t)}$ (dotted-blue) and its KMR $L(t) = \frac{2\pi}{\omega(t)} = \frac{\pi}{\omega_{\mathrm{X}}(t) + \omega_{\mathrm{Y}}(t)}$ (solid-red). The mean frequency is $\Omega = \frac{2\pi}{11}\,\mathrm{y}^{-1}$.

Figure 6. Effect of preliminary averaging on the evolution of series: sunspot number [R_I] (a), aa-index (b), sliding correlation $C(R_\mathrm{I}, \mathrm{aa})$ (c) and instantaneous period $L_{\mathrm{aa}}(t)$ (d). Windows of preliminary averaging are one year (dotted-blue), two years (dashed-green) and four years (solid-red).

Figure 7. Evolution of the instantaneous period of solar indices R_I and aa for different preliminary averaging: W=1y (a, d); W=2y (b, e) and W=4y (c, f). Left panels a-c: combined instantaneous period (blue) is compared with its KMR (red); right panel (d-f): combined instantaneous period (blue) is compared with individual instantaneous periods of R_I (cyan) and aa-indices (magenta).

Figure 8. Kuramoto model simulation performed for R_I and $\mathrm{aa_P}$-indices. (a) – mean coupling $\kappa(t)$; (b) – evolution of correlation $C_0(t) = C(R_\mathrm{I}, \mathrm{aa_P})$ (dotted blue) and its KMR $C(t) = C(X, Y)$ (red); (c) – coupling dissymmetry $\Delta\kappa(t)$; (d) – evolution of combined instantaneous period $L_0(t) = \frac{2\pi}{\omega_0(t)} = \frac{\pi}{\omega_{\mathrm{RI}}(t) + \omega_{\mathrm{aap}}(t)}$ (dotted blue) and its KMR

$L(t) = \frac{2\pi}{\omega(t)} = \frac{\pi}{\omega_X(t) + \omega_Y(t)}$ (red). Parameters of modeling are $\Delta\omega = 0.5$, $\Omega = \frac{2\pi}{11}\,\mathrm{y}^{-1}$, W=1y.

Figure 9. Effect of de-correlation on the reconstruction of the instantaneous period. Simulated series X (dotted cyan) and Y (magenta) have irregularity - (a), combined instantaneous period of KMR (red) departs from combined instantaneous period of series R_I and aa_p (dotted blue) – (b). Modeling is performed for correlation presented in Figure 8c and combined instantaneous period estimated for W=4y, $\Delta\omega = 0.5$, $\Omega = \frac{2\pi}{11}\,\mathrm{y}^{-1}$.

Figure 10. Effect of random noise in the amplitude to the instantaneous period variation. Top panel: evolution of the instantaneous period $L_X(t)$ (blue), $L_Y(t)$ (thin green), $L_0(t)$ (dashed red). Bottom panel: evolution of the phase difference. See parameters in the text of Appendix.

Figure 11. Effect of slowly oscillating amplitude to the instantaneous period variation. Top panel: synthetic series $X_0(t)$ (blue), $Y_0(t)$ (thin green). Bottom panel: evolution of the instantaneous period $L_X(t)$ (blue), $L_Y(t)$ (thin green), $L_0(t)$ (dashed red). See parameters in the text of Appendix.

Figure 1

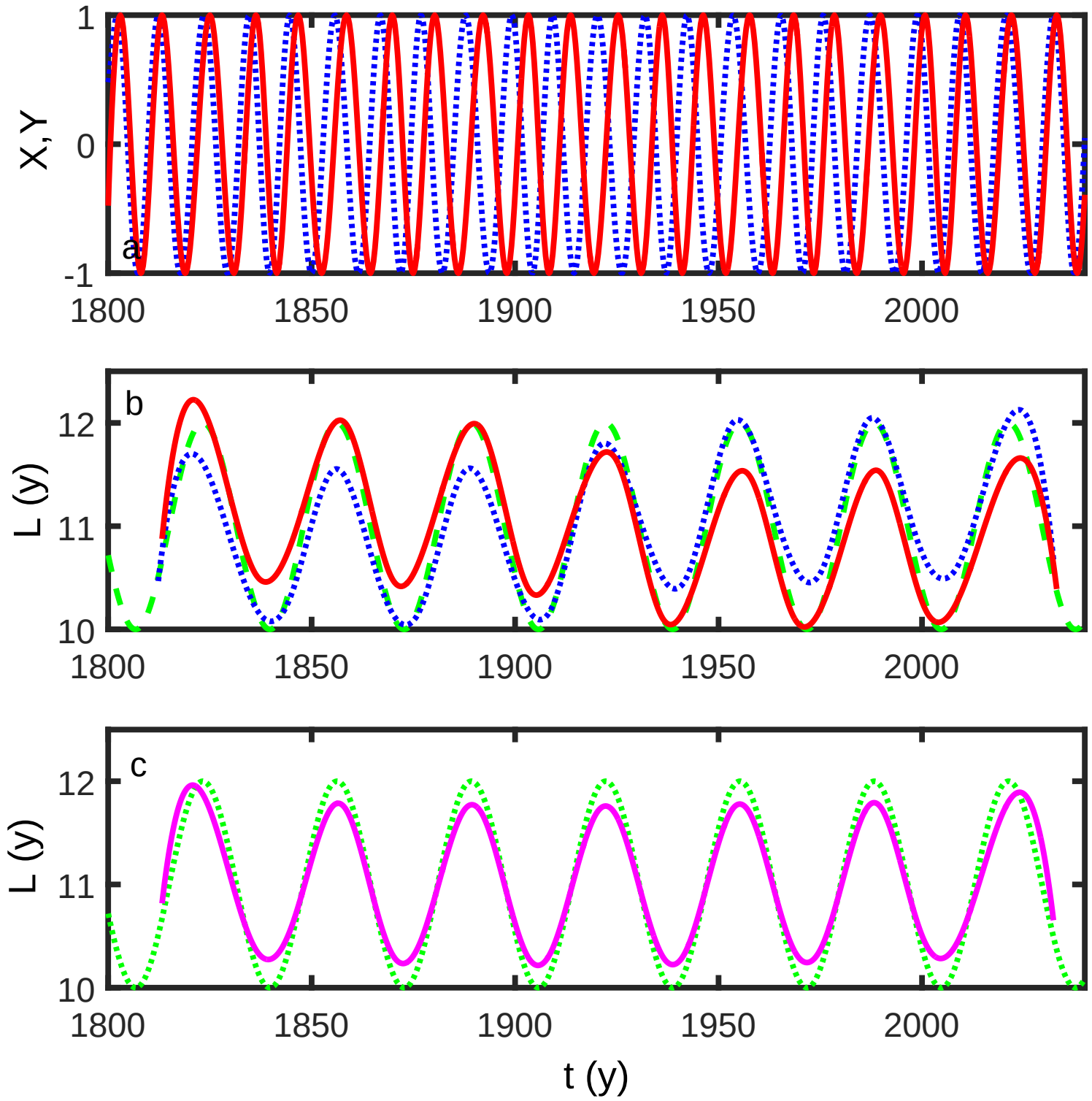
a
X, Y
1
0
-1
1800
1850
1900
1950
2000
b
L (y)
12
11
10
1800
1850
1900
1950
2000
c
L (y)
12
11
10
1800
1850
1900
1950
2000
t (y)

Figure 2

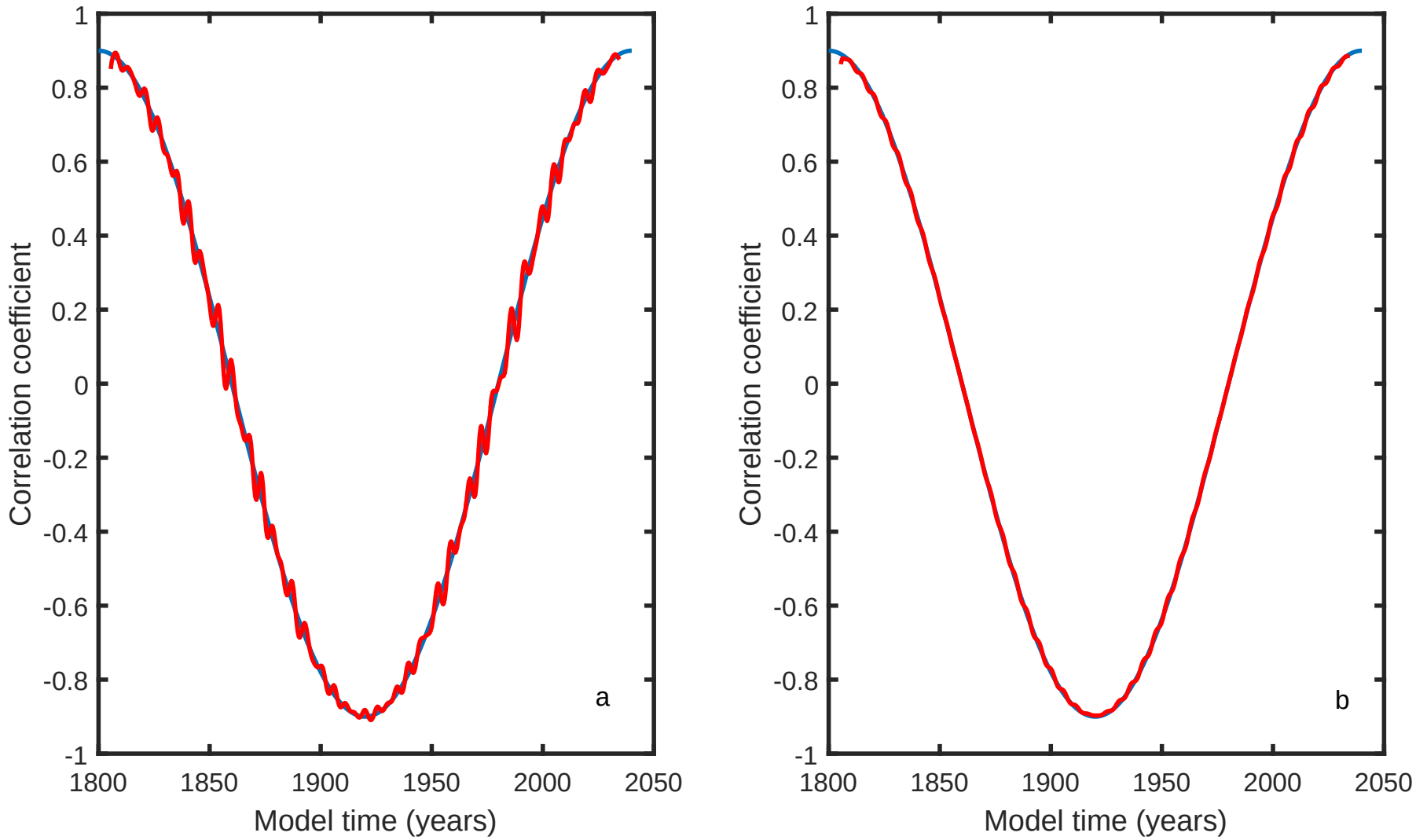
Correlation coefficient
1
0.8
0.6
0.4
0.2
0
-0.2
-0.4
-0.6
-0.8
-1
1800
1850
1900
1950
2000
2050
Model time (years)
a
b

Figure 3

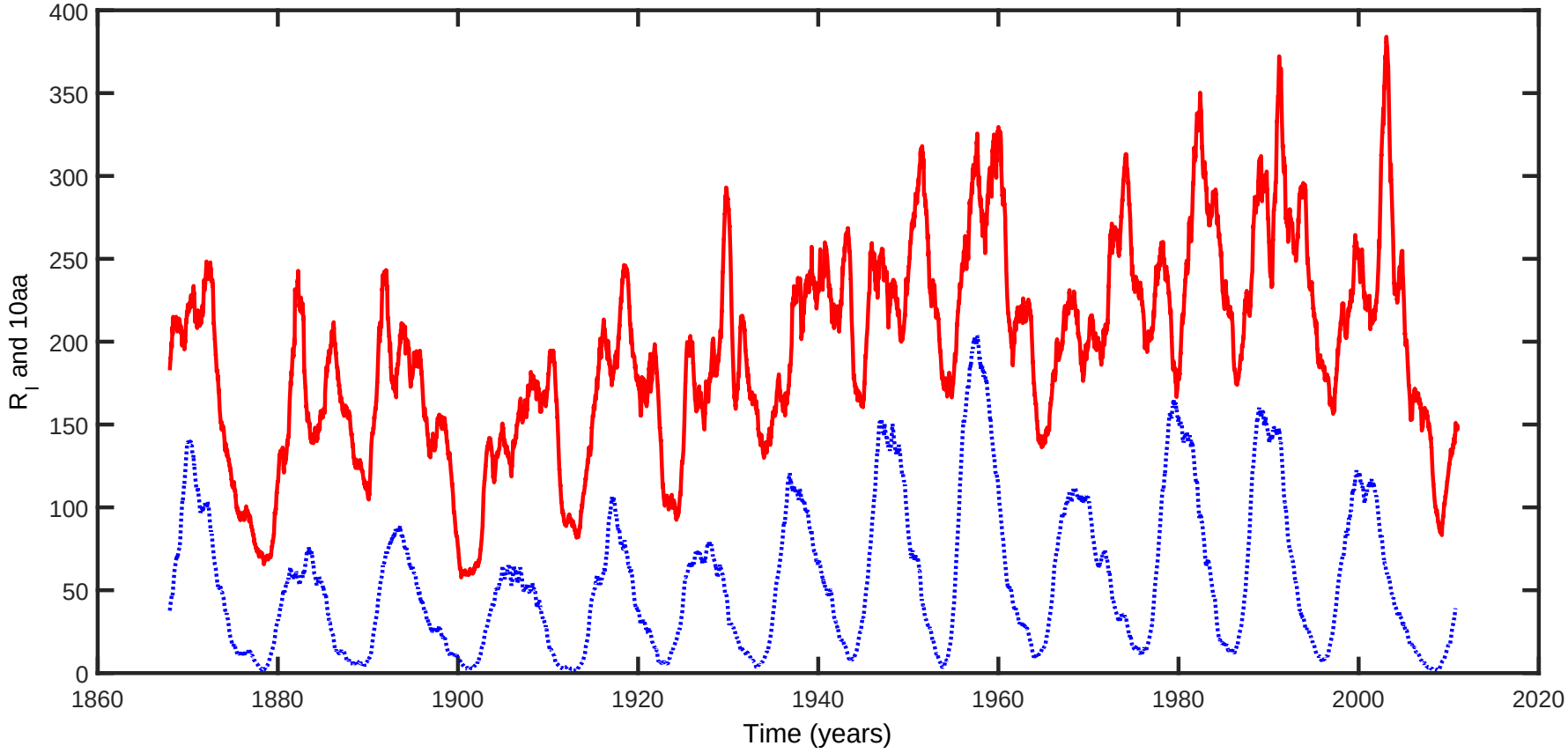
400
350
300
250
200
150
100
50
0
1860
1880
1900
1920
1940
1960
1980
2000
2020
Time (years)
R_I and 10aa

Figure 4

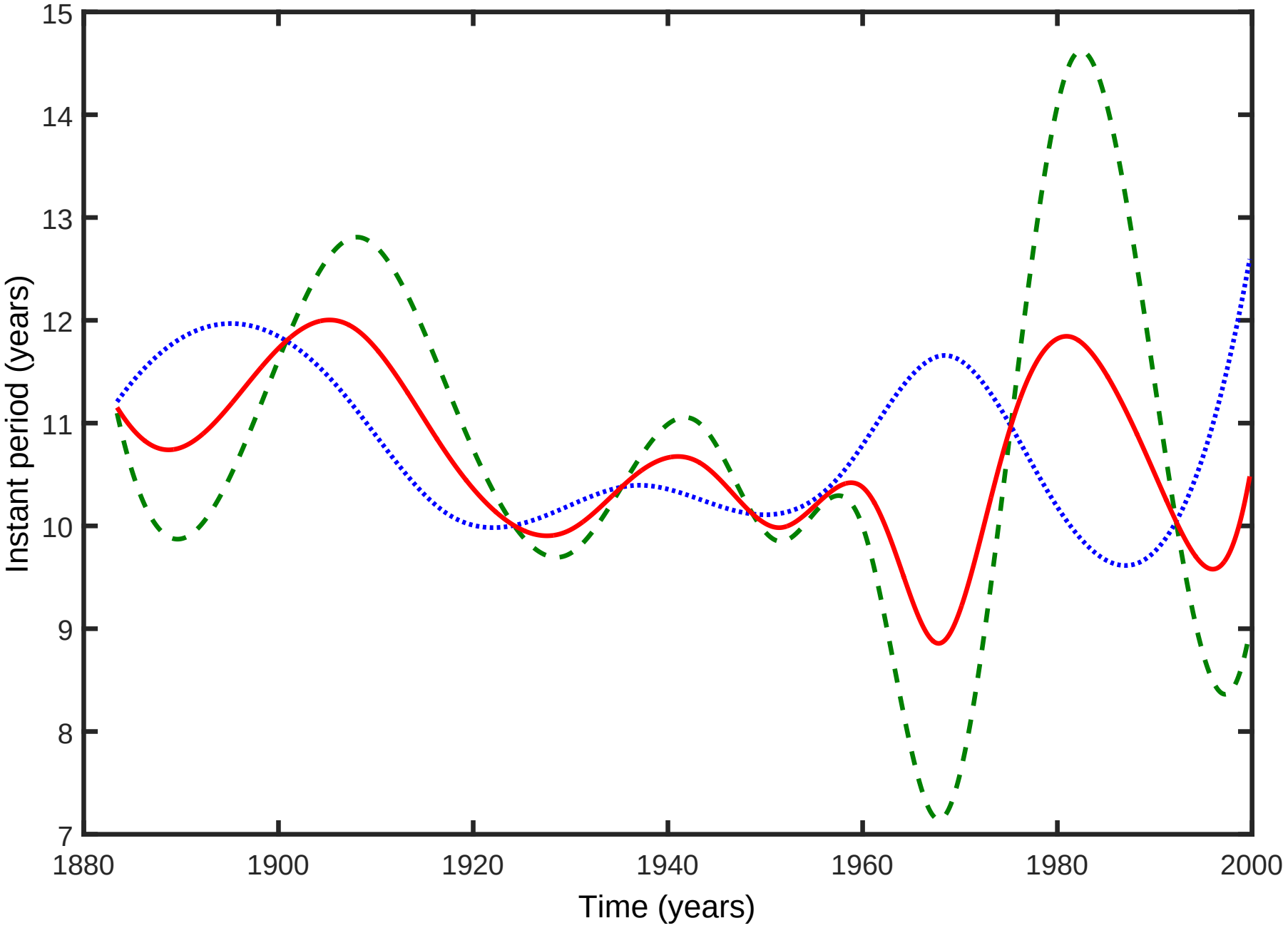
15
14
13
12
11
10
9
8
7
Instant period (years)
1880
1900
1920
1940
1960
1980
2000
Time (years)

Figure 5

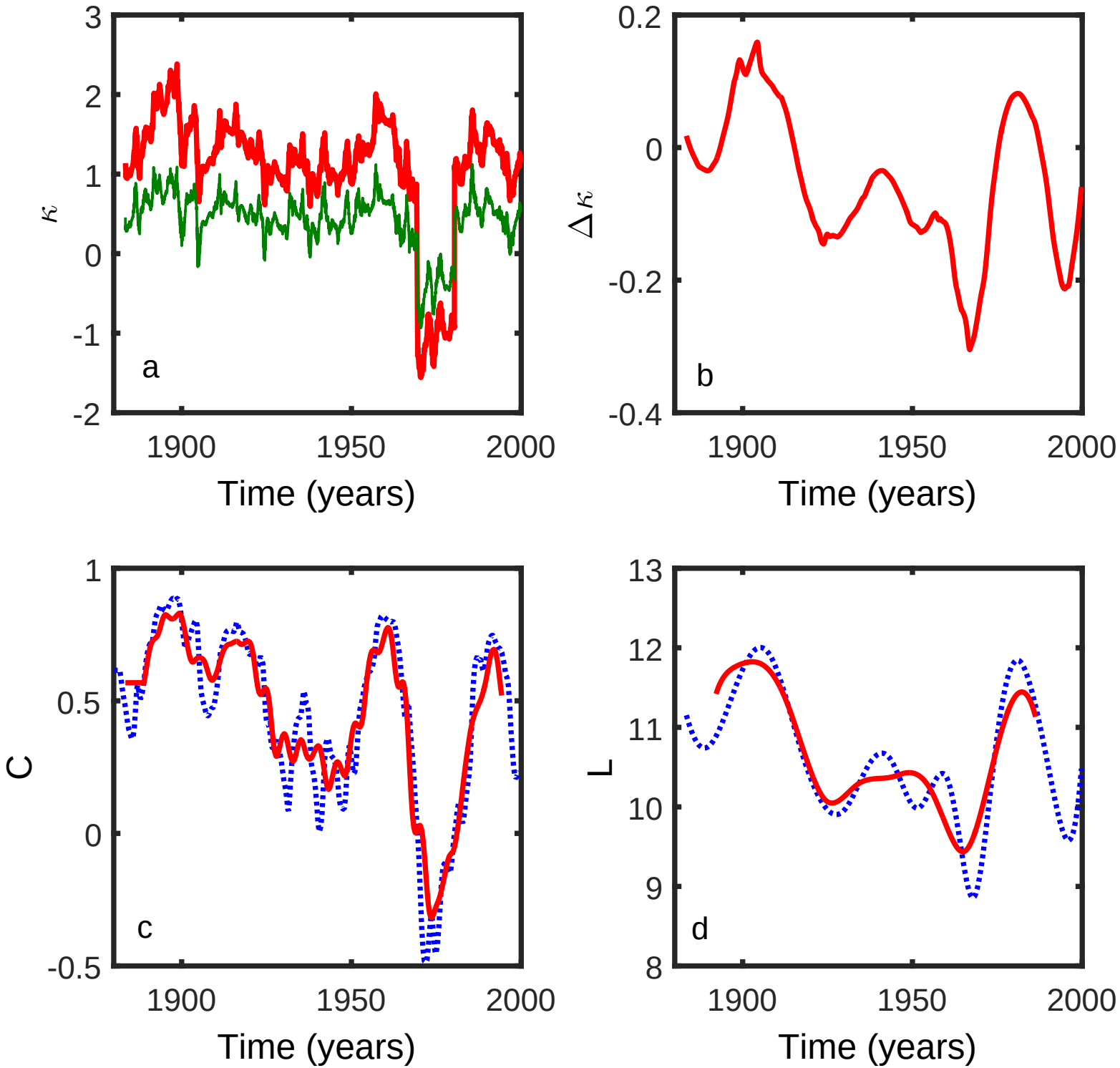
3
2
1
0
-1
-2
κ
a
1900
1950
2000
Time (years)
0.2
0
-0.2
-0.4
Δκ
b
1900
1950
2000
Time (years)
1
0.5
0
-0.5
C
c
1900
1950
2000
Time (years)
13
12
11
10
9
8
L
d
1900
1950
2000
Time (years)

Figure 6

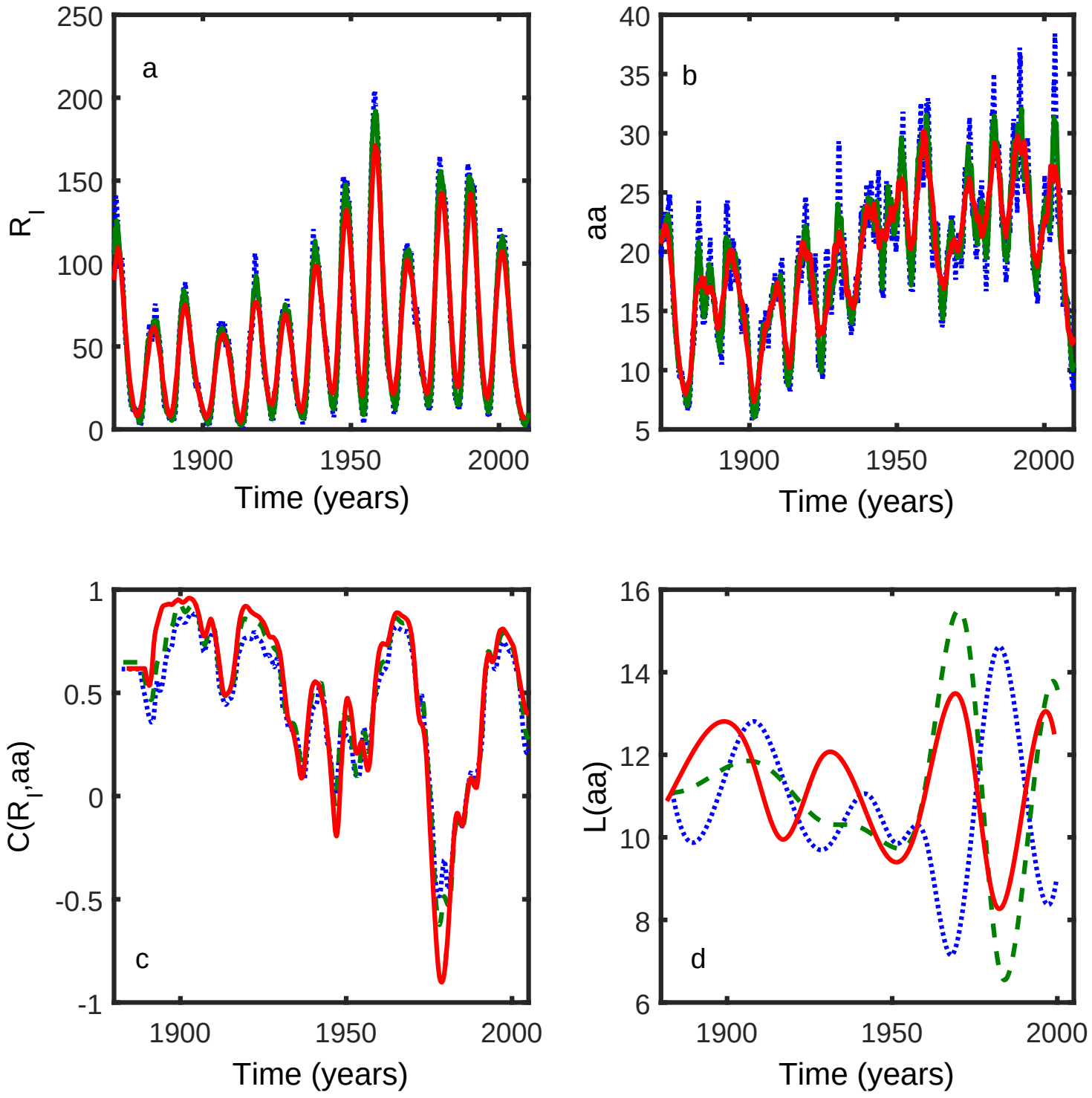
a
b
c
d
R_I
aa
$C(R_I,aa)$
L(aa)
Time (years)
Time (years)
Time (years)
Time (years)
250
200
150
100
50
0
40
35
30
25
20
15
10
5
1
0.5
0
-0.5
-1
16
14
12
10
8
6
1900
1950
2000

Figure 7

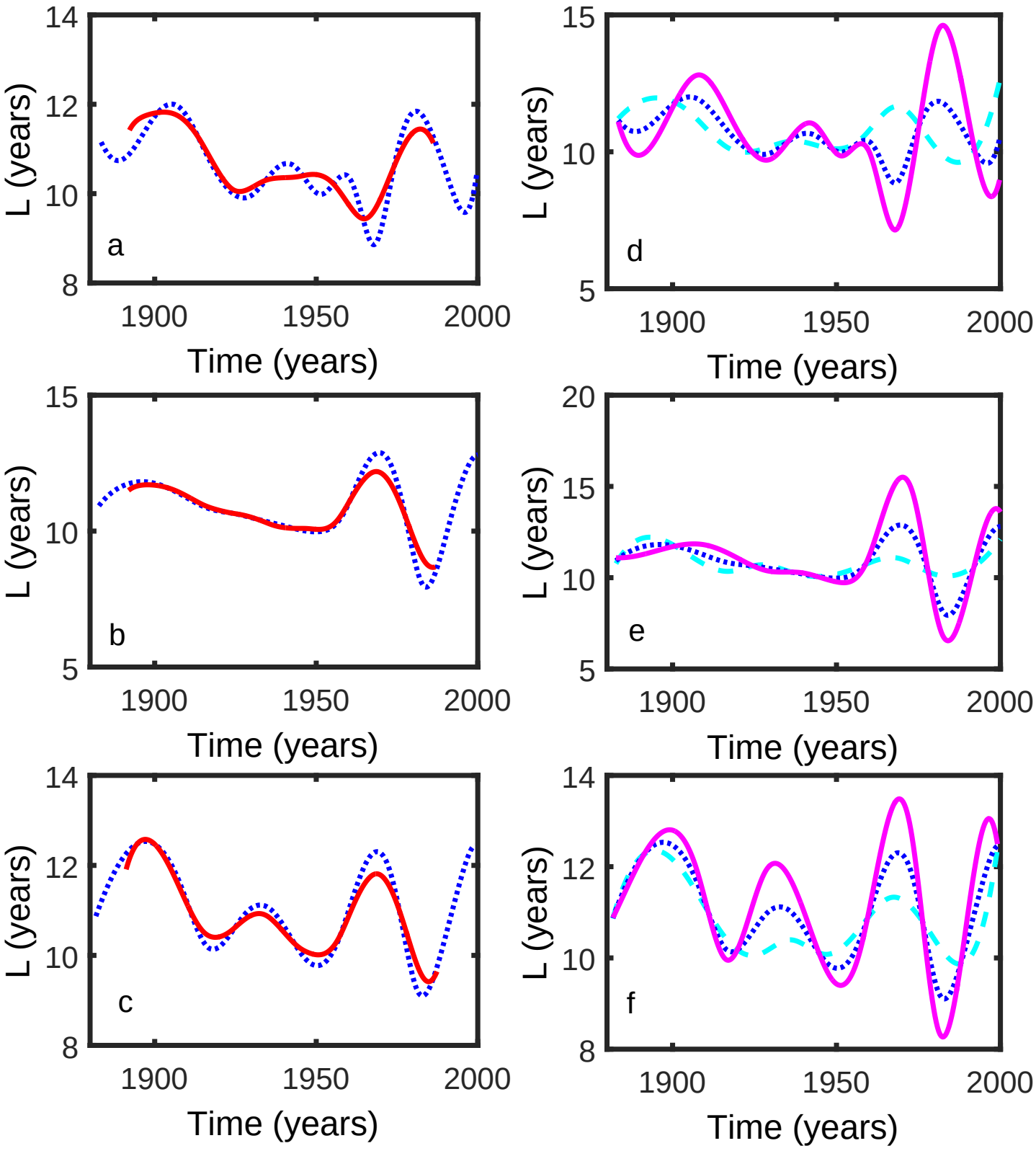

Figure 8

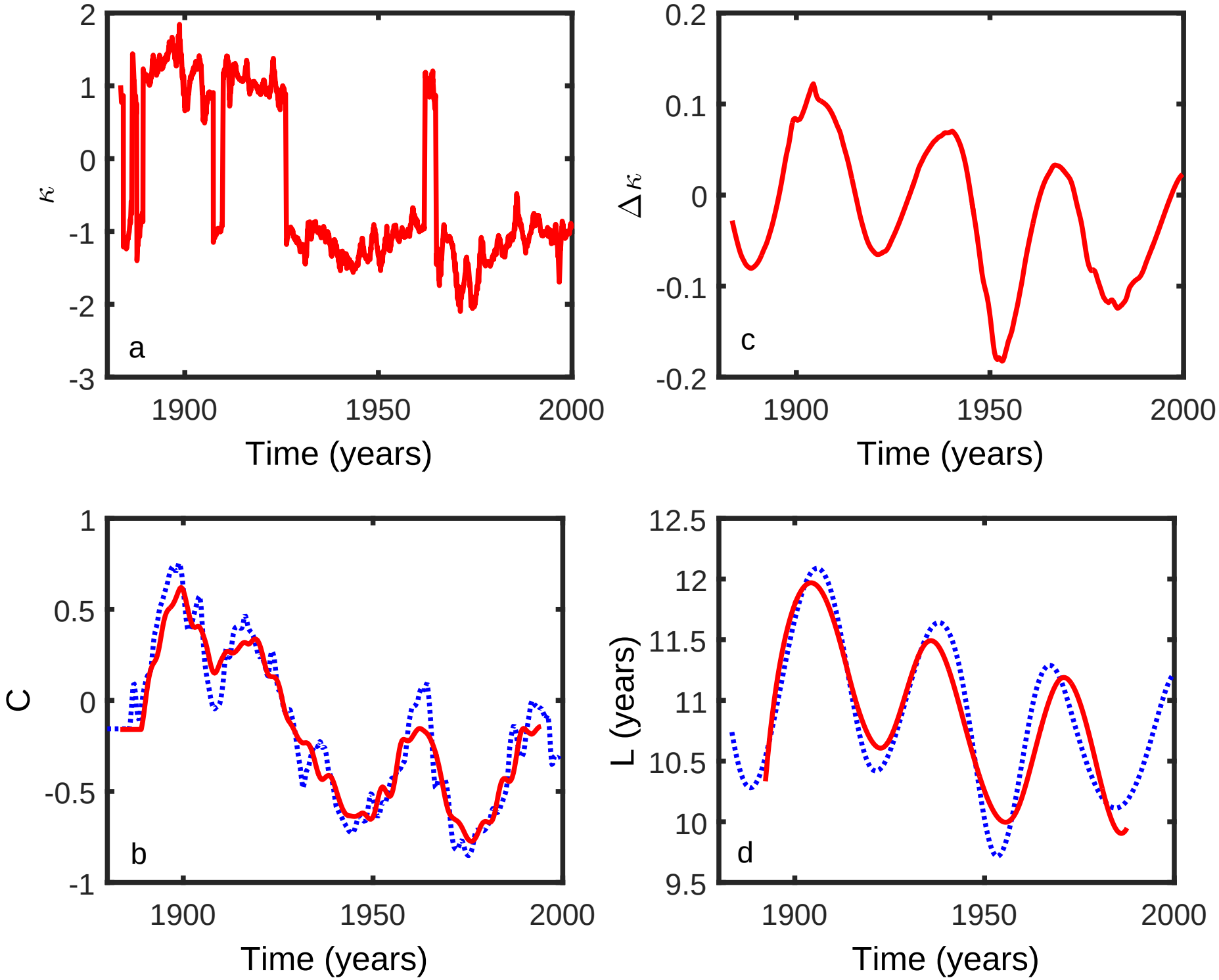
2
1
0
-1
-2
-3
κ
a
1900
1950
2000
Time (years)
0.2
0.1
0
-0.1
-0.2
Δκ
c
1900
1950
2000
Time (years)
1
0.5
0
-0.5
-1
C
b
1900
1950
2000
Time (years)
12.5
12
11.5
11
10.5
10
9.5
L (years)
d
1900
1950
2000
Time (years)

Figure 9

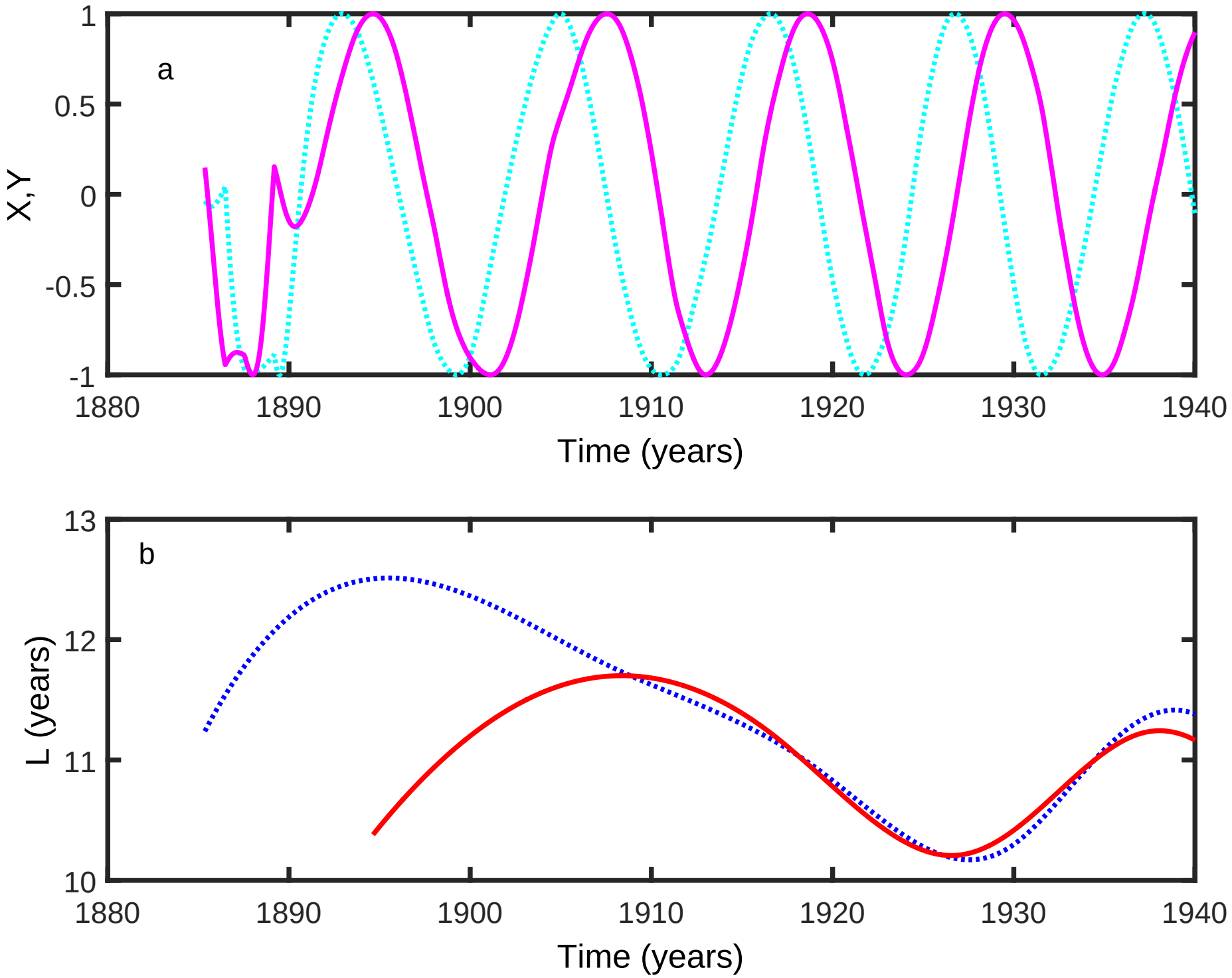
a
X,Y
1
0.5
0
-0.5
-1
1880
1890
1900
1910
1920
1930
1940
Time (years)
b
L (years)
13
12
11
10
1880
1890
1900
1910
1920
1930
1940
Time (years)

Figure 10

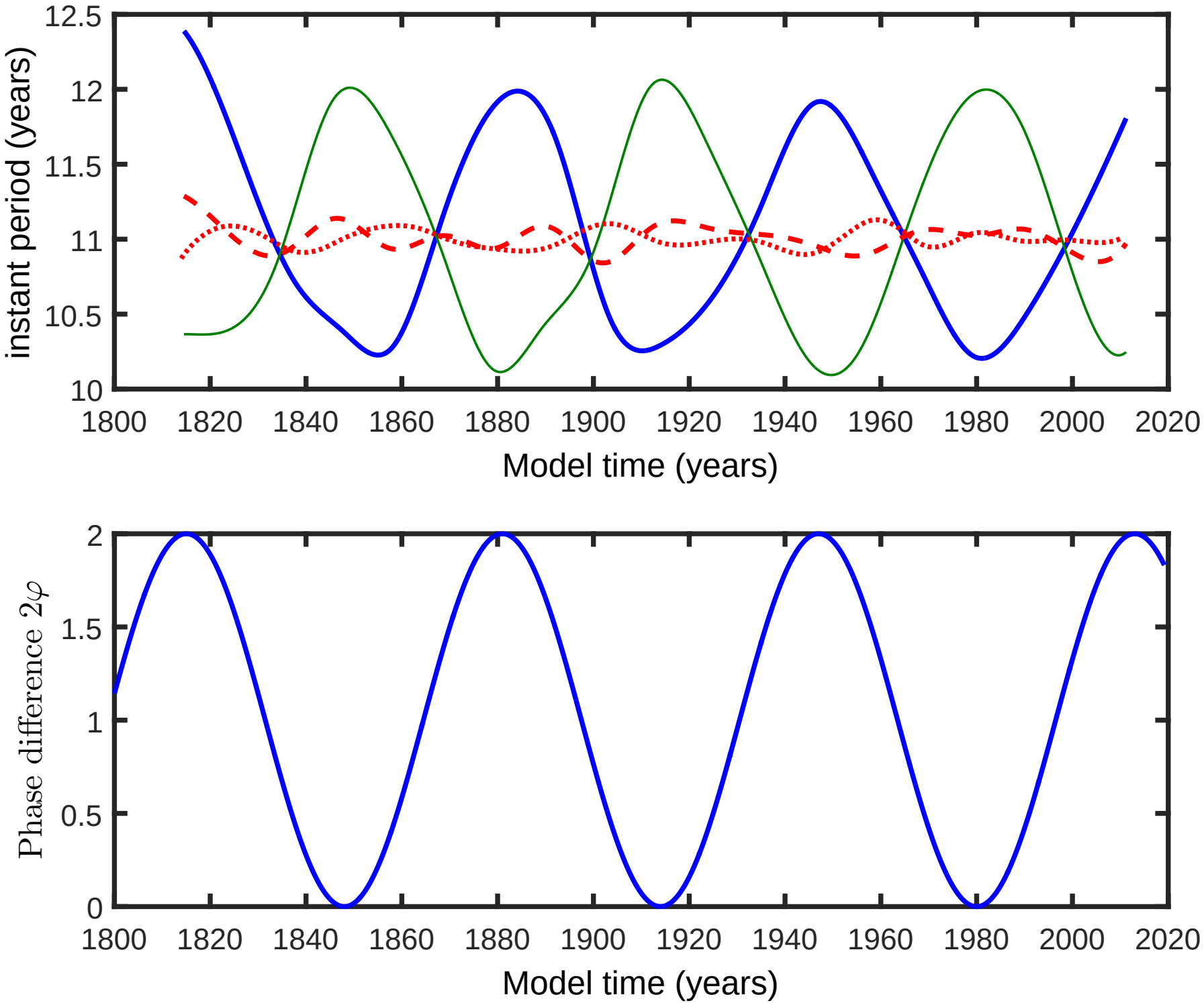
12.5
12
11.5
11
10.5
10
instant period (years)
1800
1820
1840
1860
1880
1900
1920
1940
1960
1980
2000
2020
Model time (years)
2
1.5
1
0.5
0
Phase difference 2φ
1800
1820
1840
1860
1880
1900
1920
1940
1960
1980
2000
2020
Model time (years)

Figure 11

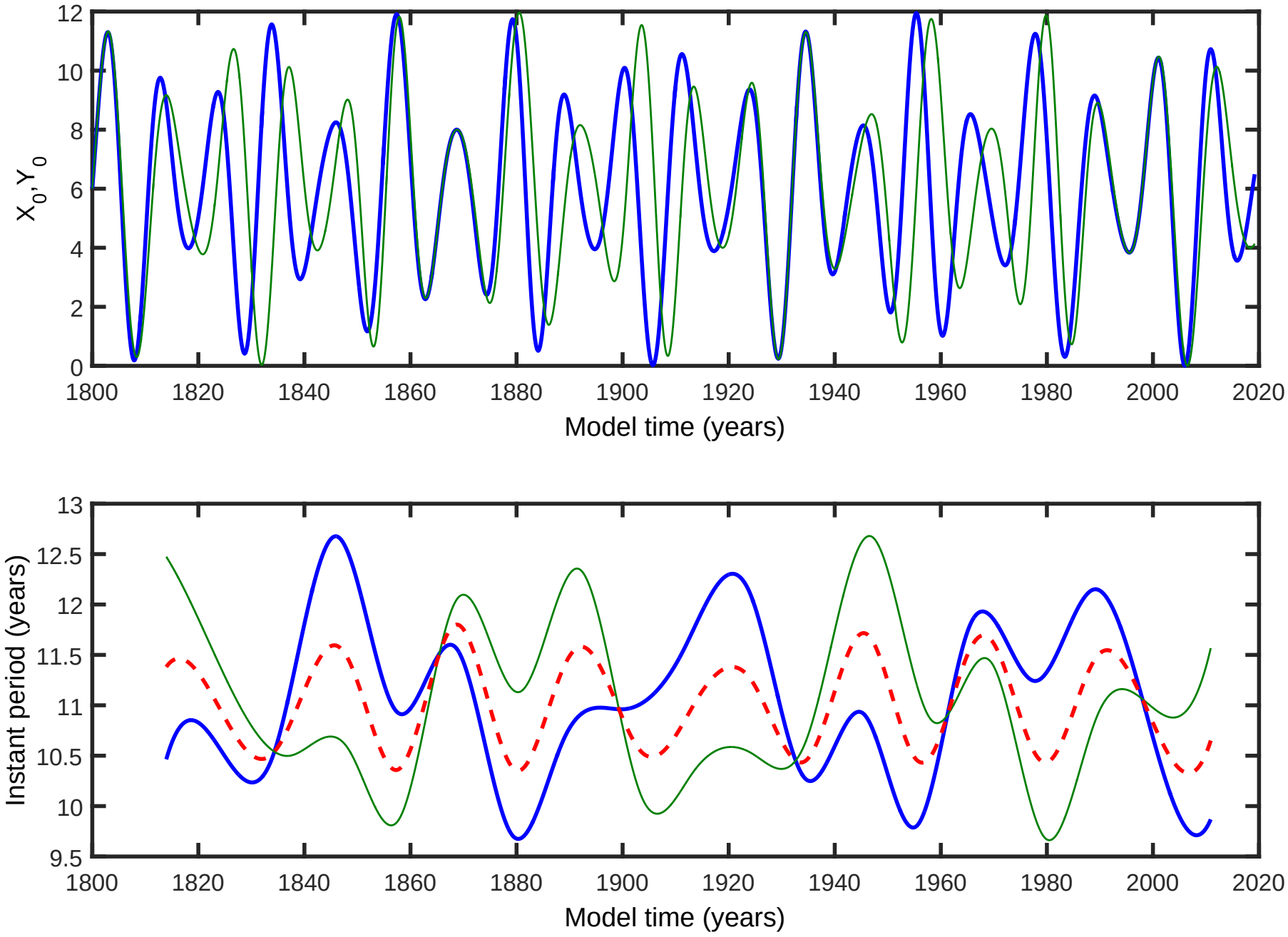
12
10
8
6
4
2
0
X_0, Y_0
1800
1820
1840
1860
1880
1900
1920
1940
1960
1980
2000
2020
Model time (years)
13
12.5
12
11.5
11
10.5
10
9.5
Instant period (years)
1800
1820
1840
1860
1880
1900
1920
1940
1960
1980
2000
2020
Model time (years)